Characterization of Methylthio-Alkane Reductase from a Novel Methionine Salvage Pathway in *Rhodospirillum rubrum*

Undergraduate Research Thesis

Presented in partial fulfillment of the requirements for graduation "with Honors Research Distinction in Molecular Genetics" in the undergraduate colleges of The Ohio State University

by
Kathryn Byerly

The Ohio State University
April 2021

Project Advisors: Dr. F. Robert Tabita, Department of Microbiology (Deceased), Succeeded by Dr. Harold Fisk, Department of Molecular Genetics

Acknowledgements

I would like to thank all of the scientists that were involved in the data collection and analysis in this study. I would like to extend appreciation to all of the collaborators from the Department of Microbiology at The Ohio State University: Justin North, Guanqi Zhao, Sarah Young, Srividya Murali, John Wildenthal, and F. Robert Tabita. Our collaborators from the Department of Soil and Crop Sciences at Colorado State University: Adrienne Narrowe and Kelly Wrighton. Our collaborators from the Chemical Sciences Division at Oak Ridge National Laboratory: Weili Xiong and Robert Hettich. Our collaborator at Pacific Northwest National Laboratory: William Cannon. Lastly, I would especially like to thank Justin North for serving as my research mentor throughout my undergraduate research experience as well as my project mentor as I completed my undergraduate thesis.

Table of Contents

Preface: Introduction to Microbial Sulfur Salvage

Sulfur is required for many cellular processes. Typically sulfur assimilation by bacteria is performed through sulfate reduction to sulfide and incorporation into cysteine[1]. Cysteine is a precursor to many essential sulfur-containing compounds—particularly methionine. When sufficient sulfate is unavailable, however, terrestrial and marine bacteria can acquire sulfur from organic sulfur compounds via methionine-salvage pathways (MSPs). Several MSPs are dedicated to recycling the metabolic byproduct 5'-methylthioadenosine (MTA) back to methionine[1,6,18]. MTA is formed when methionine derivative, *S*-adenosyl-L-methionine (SAM), is utilized for essential cell signaling processes such as polyamine synthesis and quorum sensing[17].

Understanding of the diversity of bacterial sulfur-salvage pathways has advanced recently with the discovery of new MSPs involving novel proteins and reactions. The first MSP discovered was the oxygen-dependent Universal MSP, which is utilized by most eukaryotes and many prokaryotes to recycle MTA back to methionine[1] (Figure 1, enzymes highlighted in yellow). For nearly 30 years this was thought to be the only MSP for MTA until the discovery of alternate MSPs that utilized RuBisCO and RuBisCO-like proteins (RLPs)[1]. One such MSP is the MTA-isoprenoid shunt discovered in *Rhodospirillum rubrum*[6]. The first two enzymatic steps of the MTA-isoprenoid shunt, during which MTA is converted to 5-methylthio-ribulose-1-phosphate, are analogous to the Universal MSP. The succeeding steps, however, are different with the MTA-isoprenoid shunt using a methylthioribulose-1-phosphate 1,3-isomerase from the RLP Deep-Ykr clade and a Cupin-family methylsulfurylase (Figure 1, enzymes highlighted in green). Unlike the key dioxygenase of the Universal MSP, the novel RLP isomerase and Cupin-family methylsulfurylase are oxygen-independent, making the MTA-isoprenoid shunt the first

oxygen-independent MSP discovered[6]. The key enzyme of the Calvin-Benson-Bassham cycle, RuBisCO, also participates in a distinct MSP, which through unknown mechanisms at present leads to the production of methionine precursors, *S*-methylpyruvate and *S*-methylcysteine[5] (Figure 1, enzymes highlighted in blue).

Central to this study is a recently identified oxygen-independent MSP by the F. R. Tabita lab, the Dihydroxyacetone phosphate—ethylene shunt. This MSP is characterized by the formation of dihydroxyacetone phosphate (DHAP) and ethylene in route to regenerating methionine and does not utilize a RuBisCO-family protein[18,20] (Figure 2). The DHAP—ethylene shunt is composed of two key components, the DHAP shunt and the anaerobic ethylene pathway. The DHAP shunt is a pathway composed of three enzymes that converts MTA to (2-methylthio)acetaldehyde. MTA is first phosphorylated to 5-methylthioribose-1-phosphate by MtnP, then isomerized to 5-methylthioribulose-1-phosphate by MtnA, and finally, via Ald2, a type II aldolase, is cleaved to form DHAP and (2-methylthio)acetaldehyde. In organisms *R. rubrum, Rhodopseudomonas palustris,* and extraintestinal pathogenic *E. coli* for which the DHAP shunt has been characterized, (2-methylthio)acetaldehyde is then reduced via a presumptive alcohol dehydrogenase to produce the volatile organic sulfur compound, (2-methylthio)ethanol (MT-EtOH) (Figure 2)[18,20]. The genes for the DHAP shunt are widespread, being present in 10% of sequenced bacteria, and are prevalent in freshwater, soil, and human pathogenic species[18]. Surprisingly, during studies in the Tabita laboratory of the DHAP Shunt MSP in freshwater and soil bacteria, *R. rubrum* and *R. palustris*, it was discovered that copious amounts of ethylene were produced from MT-EtOH en route to methionine[18]. This new process was named the anaerobic ethylene pathway (Figure 2). The genes and gene products responsible

for the conversion of MT-EtOH to ethylene and ultimate regeneration of methionine, however, remained unknown and are the focus of this study.

Ethylene is a plant hormone, involved in root elongation, shoot extension, leaf abscission, and fruit ripening[12]. Ethylene is natively made by plants to regulate these processes, but it can also be routinely produced by microorganisms in oxygen-depleted soils, accumulating to levels inhibitory to plant growth[23]. Thus, the DHAP—ethylene pathway has potential involvement in or impact on agricultural crop yield. Ethylene is also the highest volume industrial chemical currently produced from fossil fuels[18]. Ethylene is industrially made by steam cracking ethane, propane, or naptha (separated from natural gas and crude oil) at high temperatures[2]. Therefore, the identification of the relevant genes and isolation of the gene products in the DHAP—ethylene pathway could have application in the biological production of industrially relevant gases to decrease reliance on fossil fuels. Thus, identifying and characterizing the genes and gene products participating in the DHAP—ethylene pathway is critical for both potentially engineering the pathway for industrial ethylene production as well as understanding its functionality in environmental and pathogenic bacteria in relation to human health. The goal of this study was to identify and characterize the unknown genes and gene products of the anaerobic ethylene pathway and thus fully define the DHAP—ethylene shunt MSP of *R. rubrum*. A four-gene cluster was identified and characterized that corresponds to a putative enzyme complex from the nitrogenase superfamily that functions as a methylthio-alkane reductase. The reductase is required for the conversion of MT-EtOH to ethylene and ultimate regeneration of methionine in the DHAP—ethylene pathway.

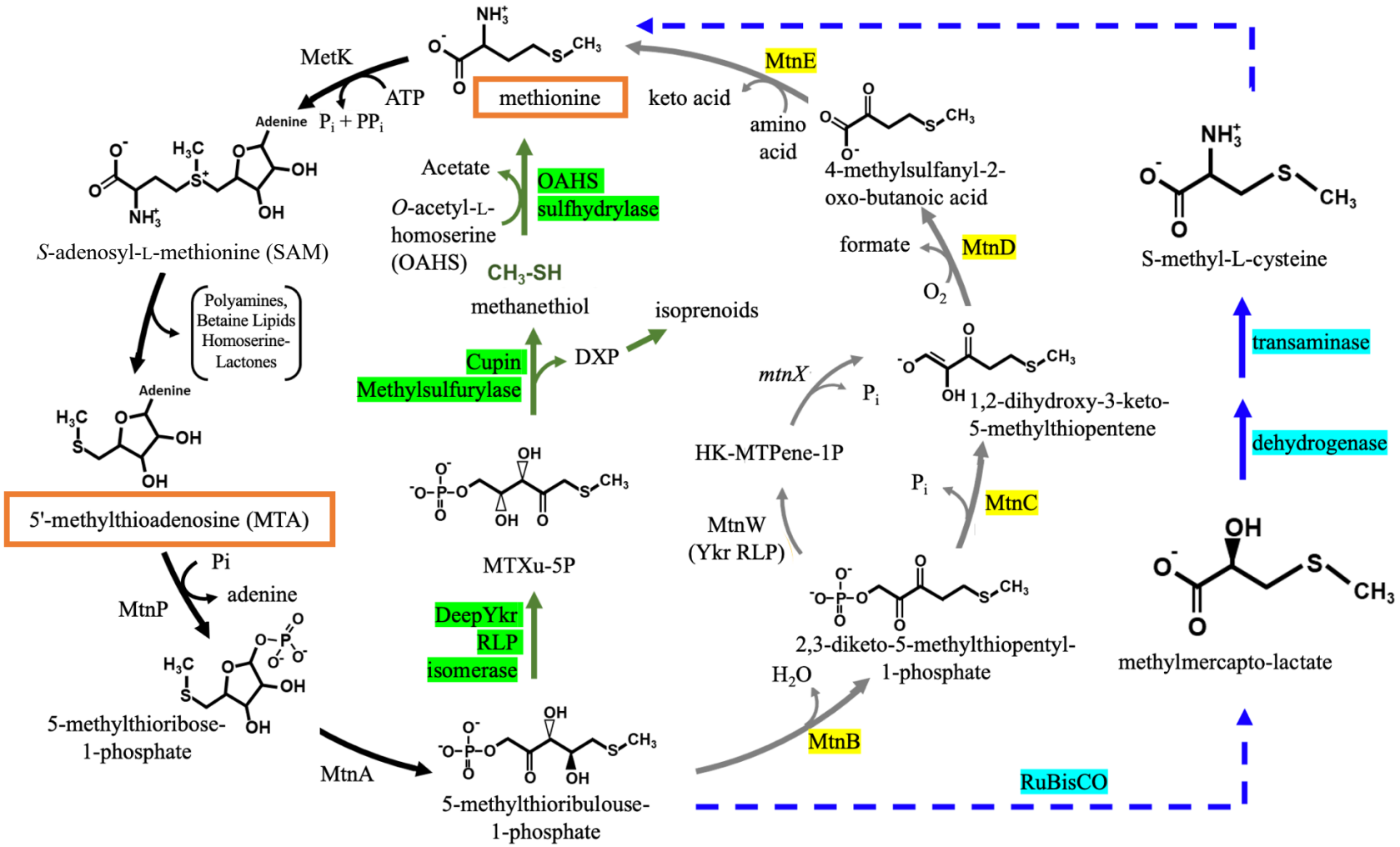

Figure 1: Pictorial representation of methionine salvage pathways. Organisms that use SAM as a substrate for quorom sensing compound and polyamine synthesis produce MTA (outlined in orange box), an inhibitory byproduct that is recycled back to methionine (outlined in orange box) via methionine salvage pathways. Enzymes unique to the Universal MSP are highlighted in yellow. Enzymes unique to the MTA-isoprenoid shunt are highlighted in green. Enzymes unique to the RuBisCO-dependent MSP are highlighted in blue.

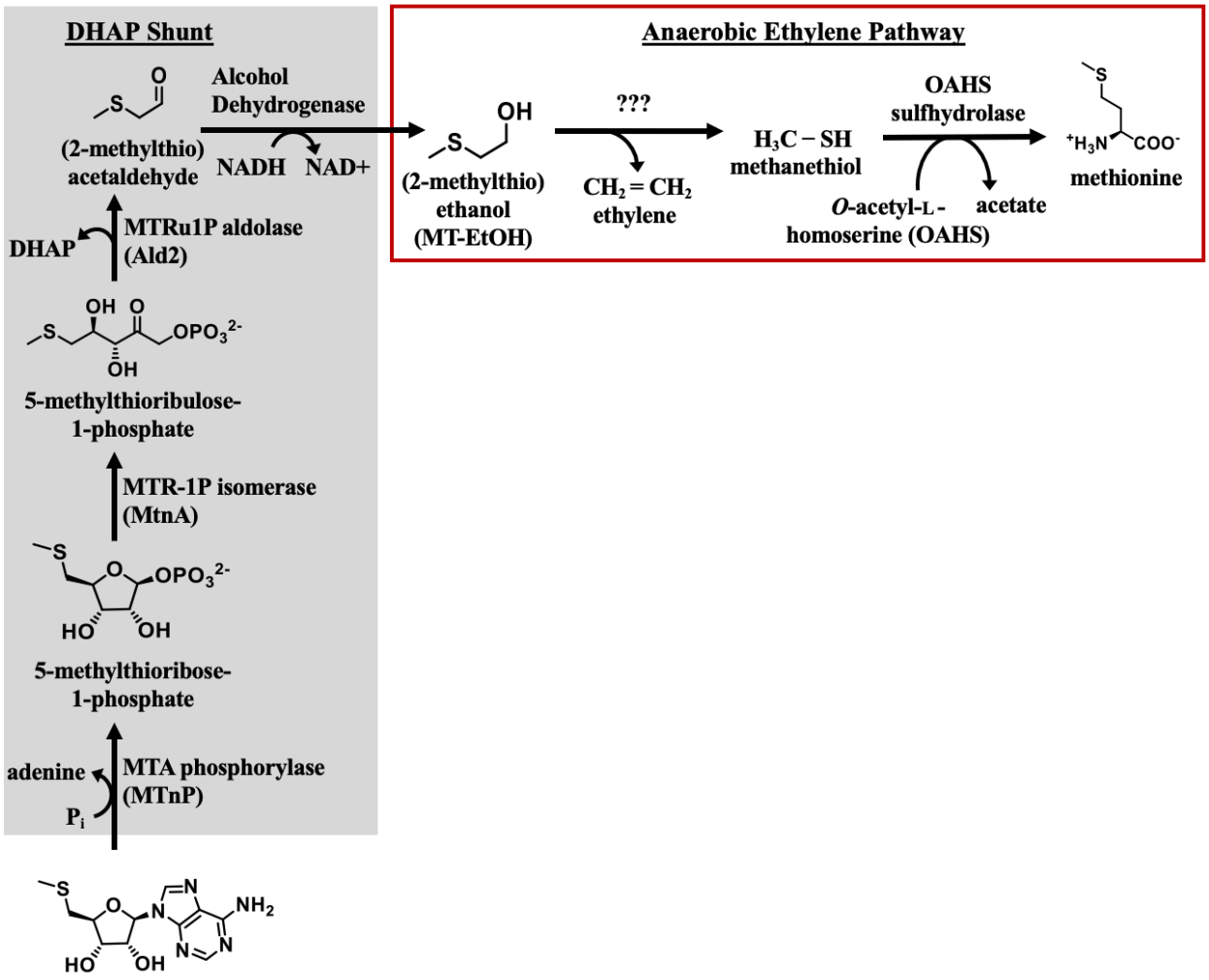

Figure 2: Pictorial representation of the the full DHAP—ethylene shunt (DHAP shunt and anaerobic ethylene pathway). The DHAP Shunt, in the gray box, recycles MTA to (2-methylthio)acetaldehyde which enters the proposed anaerobic ethylene pathway following reduction via an alcohol dehydrogenase. In the red box is the anaerobic ethylene pathway with previously unknown enzymatic steps indicated with question marks. Identification of the unknown genes and gene products responsible for ethylene synthesis and completion of the DHAP—ethylene shunt is the subject of this study.

Chapter 1: Identification of genes *marBHDK*

Material and Figures reproduced with permission from:

North, J.A., Narrowe, A.B., Xiong, W., Byerly, K.M., Zhao, G., Young, S.J., Murali, S., Wildenthal, J.A., Cannon, W.R., Wrighton, K.C., Hettich, R L., Tabita, F.R. (2020) A nitogenase-like enzyme system catalyzes methionine, ethylene, and methane biogenesis. *Science, 369*(6507), 1094-1098. doi:10.1126/science.abb6310

Chapter I Introduction

It was observed during studies of the DHAP shunt in the Tabita laboratory that stoichiometric amounts of ethylene were produced from MT-EtOH en route to methionine by a previously uncharacterized pathway[18]. In the proposed anaerobic ethylene pathway, MT-EtOH is putatively reduced via methylthio-alkane reductase activity to methanethiol, a methionine precursor (Figure 2). The genes and proteins responsible for this reduction, however, remained unknown. Thus, the first goal of this study was to determine the genes involved in the anaerobic ethylene pathway.

In preliminary experiments in the Tabita laboratory in collaboration with Dr. Bob Hettich at Oak Ridge National Laboratory, proteomic data analysis was performed. The proteomics analysis revealed which proteins exhibited increased abundance when *R. rubrum* was grown on MT-EtOH versus sulfate as a sole sulfur source (Figure 3). When grown using sulfate as the sole sulfur source, MSPs are theoretically downregulated because essential sulfur can be assimilated via sulfate reduction and incorporation into cysteine[1]. When grown using MT-EtOH, however, use of MSPs such as the DHAP—ethylene pathway is required for sulfur acquisition. Thus, requisite MSPs are likely upregulated when grown on MT-EtOH. Proteins with increased abundance in the presence of MT-EtOH versus sulfate in the proteomic data analysis were

selected for potential involvement in the anaerobic ethylene pathway. The identified genes corresponding to most of the proteins with increased abundance resided within a larger cluster of genes known to be involved in sulfur and methionine metabolism[6].

The gene clusters selected were Rru_A0772-Rru_A0773 and Rru_A0793-Rru_A0796. The proteins corresponding to genes Rru_A0772 and Rru_A0773 increased in abundance 440- and 940-fold, respectively, when grown on media supplemented with MT-EtOH versus sulfate. Proteins corresponding to genes Rru_A0793-Rru_A0796 increased in abundance 1291-, 1486-, 114-, and 121-fold, respectively. The increase in protein abundance corresponding to these genes was over three orders of magnitude higher compared to the surrounding genes (Figure 2). Surprisingly, these gene clusters were previously classified as nitrogenase fixation-like (Nfl) genes of unknown function[19]. In addition to these Nfl proteins, proteins associated with iron-sulfur metabolism also exhibited an increase in abundance. Iron-sulfur clusters (including the Nitrogenase P-clusters and M-clusters) are used by bona fide nitrogenases to act as electron carriers to transfer electrons to the nitrogen substrate[10]. Thus, involvement of the gene clusters Rru_A0772-Rru_A0773 and Rru_A0793-Rru_A0796 in the anaerobic ethylene pathway was of significant interest because it suggested Nfl complexes participate in sulfur metabolism.

To determine the putative involvement of each gene cluster and corresponding gene products in the DHAP—ethylene pathway, non-polar gene cluster deletions were performed in *R. rubrum*. Loss of growth and / or ethylene production when grown in liquid media supplemented with MT-EtOH as the sole sulfur source would implicate the involvement of the unknown gene product(s) in the anaerobic ethylene pathway. To verify if all or part of the gene cluster was critical to the function of the anaerobic ethylene pathway, subsequent complementation studies were performed using various gene combinations in *R. rubrum* expressed from a plasmid. To test

substrate specificity and alternate functions of the anaerobic ethylene pathway, additional volatile organic sulfur compounds, (methylsulfanyl)ethane (common name; ethyl methyl sulfide, EMS) and (methylsulfanyl)methane (common name; dimethyl sulfide, DMS), were supplemented in the media during the growth studies and products analyzed via gas chromatography.

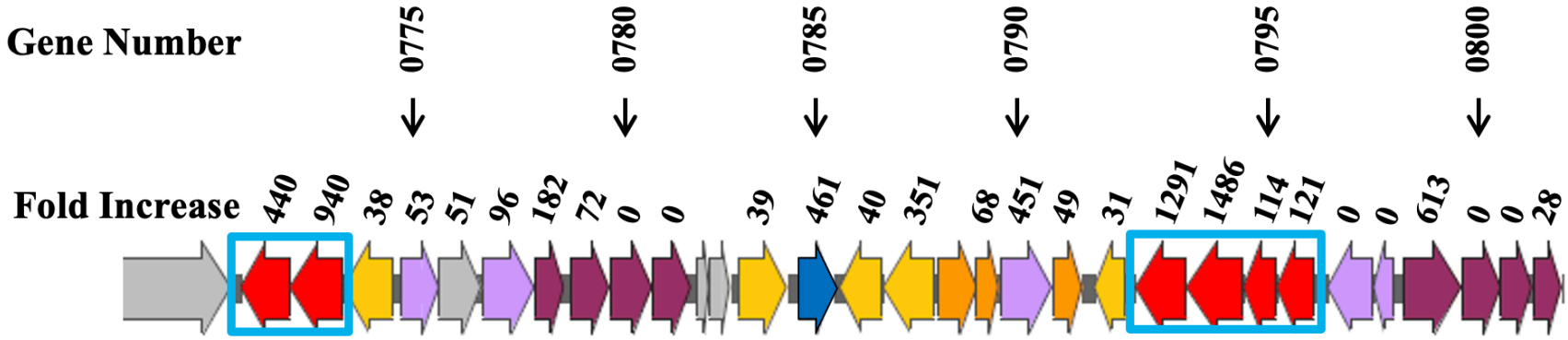

Figure 3: Proteomic data analysis of *R. rubrum* grown with MT-EtOH versus sulfate, performed by Dr. Bob Hettich. Organization of genes from the annotated *R. rubrum* genome[12] corresponding to proteins and their associated change in abundance from proteomic analysis. Fold increase is the average amount the corresponding protein increased in abundance from three independent trials when *R. rubrum* was grown on media supplemented with 1 mM MT-EtOH versus 1 mM sulfate. Red genes (outlined in the bright blue box) are nitrogen fixation-like genes and represent the selected gene clusters predicted to have function in the anaerobic ethylene pathway. Orange genes have predicted function in methionine transport. Yellow genes have predicted function in sulfur metabolism. Blue gene is SalR (Rru_A0785) which confers transcriptional control of methylthio-alkane reductase genes[19]. Lavender genes are of an unknown function. Maroon genes are predicted to be involved in transport of unknown function.

Chapter I Methods

Cloning Techniques and Bacterial Growth

R. rubrum ATCC 11170 wild type strain (Sm^R; NC_007643.1; American Type Culture Collection) was the background in which the gene deletions were performed. Anaerobic growth of *R. rubrum* was performed in static anaerobic culture tubes and serum bottles at 30°C with 2000 lux incandescent illumination. Anaerobic cultures were composed of sulfur-free Omerod's malate minimal media (MMM; Appendix) supplemented with the indicated sulfur source under a 95:5 mixture of N_2:H_2 gaseous headspace. Growth studies were conducted in MMM supplemented with 1 mM of the designated sulfur source. Culture density was analyzed during growth studies at an optical density (O.D.) of 660 nm.

Construction of Gene Deletion Strains

A schematic representation of the knockout of *R. rubrum* genes by homologous recombination is shown in Figure 4.

i) Construction of pK18mobSacBgm Knockout Vector

To construct the nonpolar gene deletions of Rru_A0772-Rru_A0773 (henceforth termed Δ0772:3) and Rru_A0793-Rru_A0796 (henceforth termed Δ0793:6) in the *R. rubrum* wild type strain, knockout vectors using the pK18mobSacBgm backbone were constructed for use in homologous recombination. For each of the selected gene clusters to be deleted, two sets of primers (Table 1) were designed to amplify via PCR (Appendix) 1,000 bp upstream and 1,000 bp downstream of the selected gene clusters. Each primer was designed to include compatible restriction enzyme recognition sites for subsequent digestion and ligation. The PCR products were digested with their respective restriction enzymes using manufacturer's protocols (New England Biolabs), purified using a QIAGEN PCR-cleanup kit, and ligated to one another using

T4 DNA ligase (New England Biolabs) to result in a truncated gene fragment. The pK18mobSacBgm plasmid was additionally digested with the restriction enzymes matching the restriction sites on the outside ends of the truncated gene fragment using manufacturer's protocol (New England Biolabs), treated with Antarctic phosphatase (New England Biolabs) to decrease the likelihood of plasmid recircularization during ligation, and purified using a QIAGEN PCR-cleanup kit. The truncated gene fragment and vector backbone were then ligated together using T4 DNA ligase (New England Biolabs).

ii) Transformation of *E. coli* with Knockout Vectors

Chemically-competent *E. coli* Stellar cells (TaKaRa Bio) were transformed with the pK18mobsacBgm knockout vector containing the truncated gene fragment. Five µL of ligation mixture was added to a 100 µL aliquot of chemically-competent *E. coli* Stellar cells and incubated on ice for 20 min. The mixture underwent heat shock at 42°C for 1 minute and was incubated on ice again for an additional 5 minutes. Five hundred µL of SOC liquid media (Appendix) was then added to the mixture and the culture was placed in a shaker table heated to 37°C for 1 hour. The cells were spread-plated onto lysogeny broth (LB; Appendix)—1.6% (w/v) solid agar plates with 25 µg/mL kanamycin and 30 µg/mL gentamycin. Individual colonies were picked and grown in 5 mL of LB liquid medium, and the plasmids were extracted using a QIAGEN Miniprep kit. Plasmid sequences were verified by Sanger sequencing at the Ohio State University Comprehensive Cancer Center Shared Resource Facility (OSU-CCC Shared Resources).

iii) Conjugative Transfer of Knockout Vectors into *R. rubrum*

Sequence-verified plasmids were mobilized into *R. rubrum* wild type cells by conjugative transfer using triparental mating with helper strain *E. coli* JM109/pRK2013 (American Type

Culture Collection). *R. rubrum* was initially grown aerobically at 30°C to late exponential phase in peptone yeast extract (PYE; Appendix) liquid media. Helper strain, *E. coli* JM109/pRK2013, and *E. coli* Stellar cells transformed with the knockout vectors were grown in LB liquid media at 37°C to mid exponential phase. Each strain was separately centrifuged and washed three times with PYE liquid media. Strains were combined in a 1:2:1 ratio of transformed *E. coli* Stellar cells, *E. coli* JM109/pRK2013 cells, and *R. rubrum* cells, concentrated, and spotted onto a PYE—1.6% (w/v) solid agar plate. Triparental mating was carried out aerobically at 30°C for 2 days. *R. rubrum* transconjugants were selected on PYE—1.6% (w/v) solid agar plates with 25 µg/mL kanamycin and 50 µg/mL streptomycin under aerobic growth at 30 °C. Isolates having undergone the first recombination event with the knockout vector were selected using sucrose sensitivity and 25 µg/mL kanamycin resistance. These isolates there then cultured in liquid PYE aerobically at 30°C to allow for the second recombination event to occur. Isolates having undergone the second recombination even were selected via loss of sucrose sensitivity and kanamycin resistance. Isolates were then tested for their ability to grow anaerobically in MMM supplemented with 1 mM sulfate, 1mM MT-EtOH, 1 mM EMS, or 1mM DMS as a sole sulfur source. *R. rubrum* deletion strains were also assayed for ethylene or other volatile gas production by gas chromatography as described below.

Construction of Gene Complementation Strains

A schematic representation of the plasmid-based gene complementation of the *R. rubrum* Δ0772:3/Δ0793:6 strain is shown in Figure 5.

i) Construction of pMTAP Plasmids Containing the Genes-of-Interest

To construct *R. rubrum* Δ0772:3/Δ0793:6 gene complementation strains, plasmid pMTAP-MCS3 was used to assemble distinct gene combinations of Rru_A0772-Rru_A0773 and

Rru_A0793-Rru_A0796. For each set of genes selected to be expressed in *trans* from pMTAP-MCS3 in *R. rubrum*, primers (Table 1) were designed to amplify selected genes by PCR and incorporate restriction enzyme cut sites for ligation into the pMTAP-MCS3 plasmid. The genes of interest were amplified via PCR (Appendix), digested with their respective restriction enzymes using manufacturer's protocols (New England Biolabs), and purified using a QIAGEN PCR-cleanup kit. The pMTAP-MCS3 plasmid was additionally digested with restriction enzymes matching the restriction sites on the first and last genes to be assembled into the plasmid using manufacturer's protocol (New England Biolabs), treated with Antarctic phosphatase (New England Biolabs) to reduce plasmid recircularization during ligation, and purified using a QIAGEN PCR-cleanup kit. The genes and pMTAP-MCS3 plasmid were then ligated together using T4 DNA ligase (New England Biolabs).

ii) Transformation of *E. coli* with pMTAP Complementation Plasmids

Chemically-competent *E. coli* SM10 cells[21] were transformed with the pMTAP plasmids containing the genes of interest from *R. rubrum*. Five µL of ligation mixture was added to a 100 µL aliquot of chemically-competent *E. coli* SM10 cells and incubated on ice for 20 minutes. The mixture underwent heat shock at 42°C for 1 minute and was incubated on ice again for an additional 5 minutes. Five-hundred µL of SOC media was then added to the mixture and the culture was placed in a shaker table heated to 37°C for 1 hour. The cells were then spread-plated onto LB—1.6% (w/v) solid agar plates with 25 µg/mL kanamycin and 10 µg/mL tetracycline. Individual colonies were picked and grown in 5 mL of LB liquid media with 25 µg/mL kanamycin and 10 µg/mL tetracycline, and the plasmids were extracted using a QIAGEN Miniprep kit. Plasmid sequences were verified by sequencing at the OSU-CCC Shared Resources, The Ohio State University.

iii) Conjugative Transfer of MTAP Complementation Plasmids into *R. rubrum*

Sequence-verified plasmids were mobilized by conjugative transfer into *R. rubrum* Δ0772:3/Δ0793:6 cells using biparental mating with the transformed *E. coli* SM10 cells. *R. rubrum* was initially grown aerobically at 30°C to late exponential phase in PYE liquid medium. *E. coli* SM10 transformants were grown aerobically at 37 °C to mid exponential phase in LB liquid medium. Strains were separately centrifuged and washed three times with PYE medium, combined in a 1:2 ratio of *E. coli* to *R. rubrum*, concentrated, and spotted onto a PYE—1.6% (w/v) solid agar plate. Biparental mating was carried out aerobically at 30°C for 2 days. *R. rubrum* transconjugants were selected on PYE—1.6% (w/v) solid agar plates with 2 μg/mL tetracycline and 50 μg/mL streptomycin under aerobic growth at 30°C. Isolates were then tested for their ability to grow anaerobically with sulfate, MT-EtOH, EMS, or DMS as sole sulfur source. *R. rubrum* Δ0772:3/Δ0793:6 transconjugants with plasmids that complemented for growth on MT-EtOH, DMS, and EMS were also quantified by gas chromatography for restoration of ethylene, methane, or ethane, respectively.

Gas Chromatography Analysis

Quantification of methane, ethane, and ethylene was performed using a Shimazdu GC-14A with Restek Rt-Alumina BOND/Na_2SO_4 column. Gaseous culture headspace after growth experiments as described above was injected (250 μL) at 180°C and separated isothermally at 30°C with helium as the carrier gas. Eluted compounds were detected by a flame ionization detector at 180°C and identified based on retention time of methane and ethylene standard (Praxair). The total amount of each hydrocarbon present was calculated from the peak area as compared to standard concentration curves of the corresponding reference standard.

Pairwise Alignment *R. rubrum* Rru_A0793-Rru_A0796 Gene Products with Nitrogenase Genes Performed by Dr. Justin North[17]

Pairwise alignment of NifB, NifH, NifD, and NifK nitrogenase protein sequences with *R. rubrum* Nfl proteins corresponding to gene products of Rru_A0793-Rru_A0796 for conserved amino acid residues was performed using Clustal Omega (EMBL-EBI) and visualized with Jalview.

Construction of Phylogenetic Tree of NifD Superfamily Performed by Dr. Adrienne Narrowe (reproduced from North et al.[17])

R. rubrum Rru_A0793 gene was queried against the NCBI reference genome database using the translated nucleotide blast (tblastn) algorithm and filtered for protein subjects with e-value < e-50. Each identified potential homolog to Rru_A0793 was correlated with its reference genome and only genomes were retained that contained all three homologues to Rru_A0793-Rru_A0795 on the same contig and with homologs to Rru_A0793 and Rru_A0794 being adjacent. These candidates, along with recently discovered Group VI nitrogen fixation-like representatives from metagenome assembled genomes were then appended to a reference nitrogenase (Groups I, II, III) and NFL sequence (Groups IV and V) database with additional sequences identified from genomes in the JGI IMG/M database. Amino acid sequences were aligned using MAFFT (v7.394) (--auto). Alignments were trimmed using TrimAl (v1.4.rev22) (--gappyout). Maximum likelihood trees were constructed using IQ-TREE (v1.6.8) (-alrt 1000 -bb 1000) using best-fit models (LG+R6) identified by ModelFinder as implemented in IQ-TREE with ultrafast bootstrap (UFBoot).

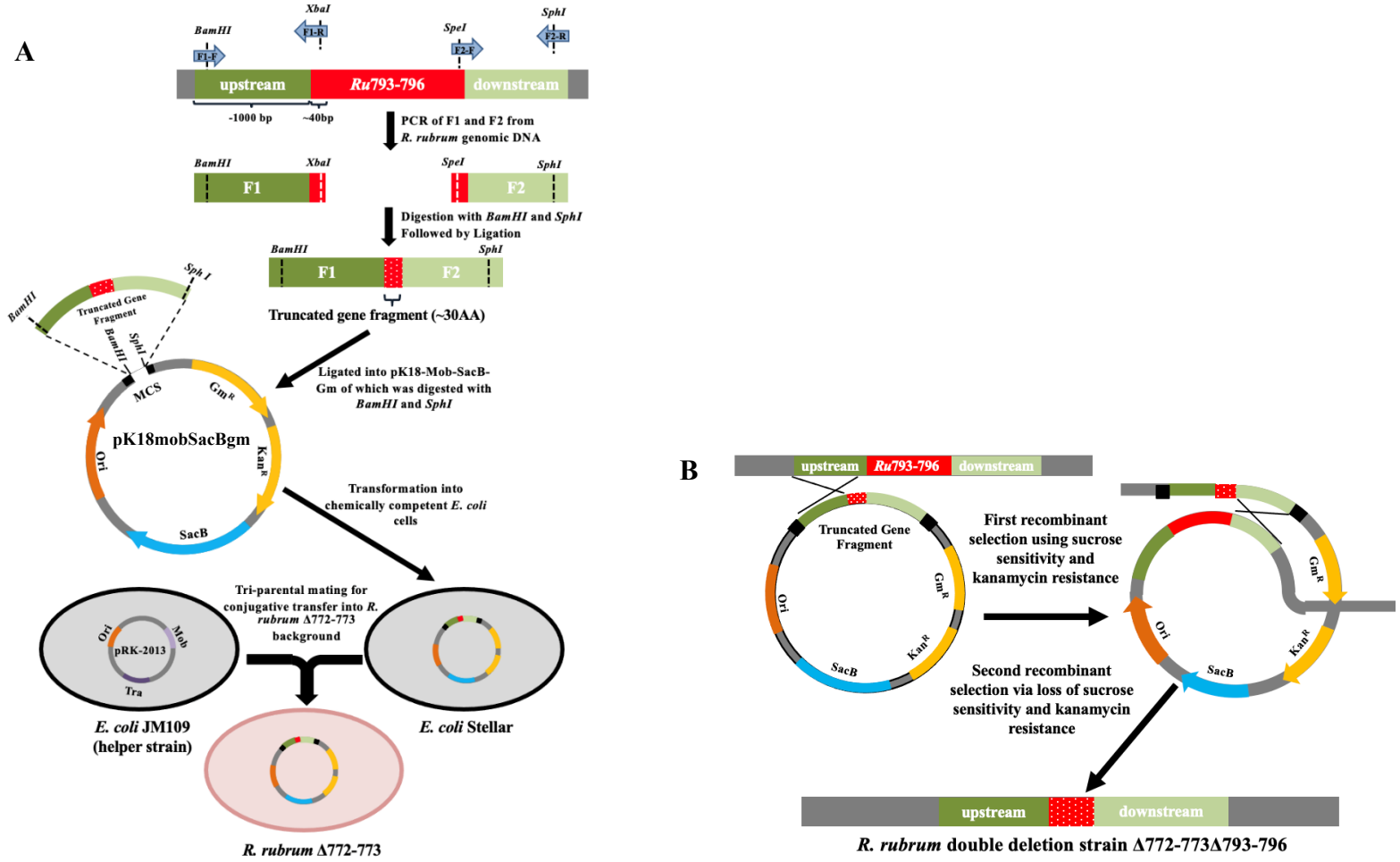

Figure 4: Schematic for knockout of putative *R. rubrum* methylthio-alkane reductase genes. Panel A illustrates the construction of the pK18mobSacBgm knockout vector and the subsequent transformation of *E. coli* cells and conjugative transfer to *R. rubrum* wild type cells. Panel B illustrates the chromosomal integration via homologous recombination that resulted in the gene deletion strains.

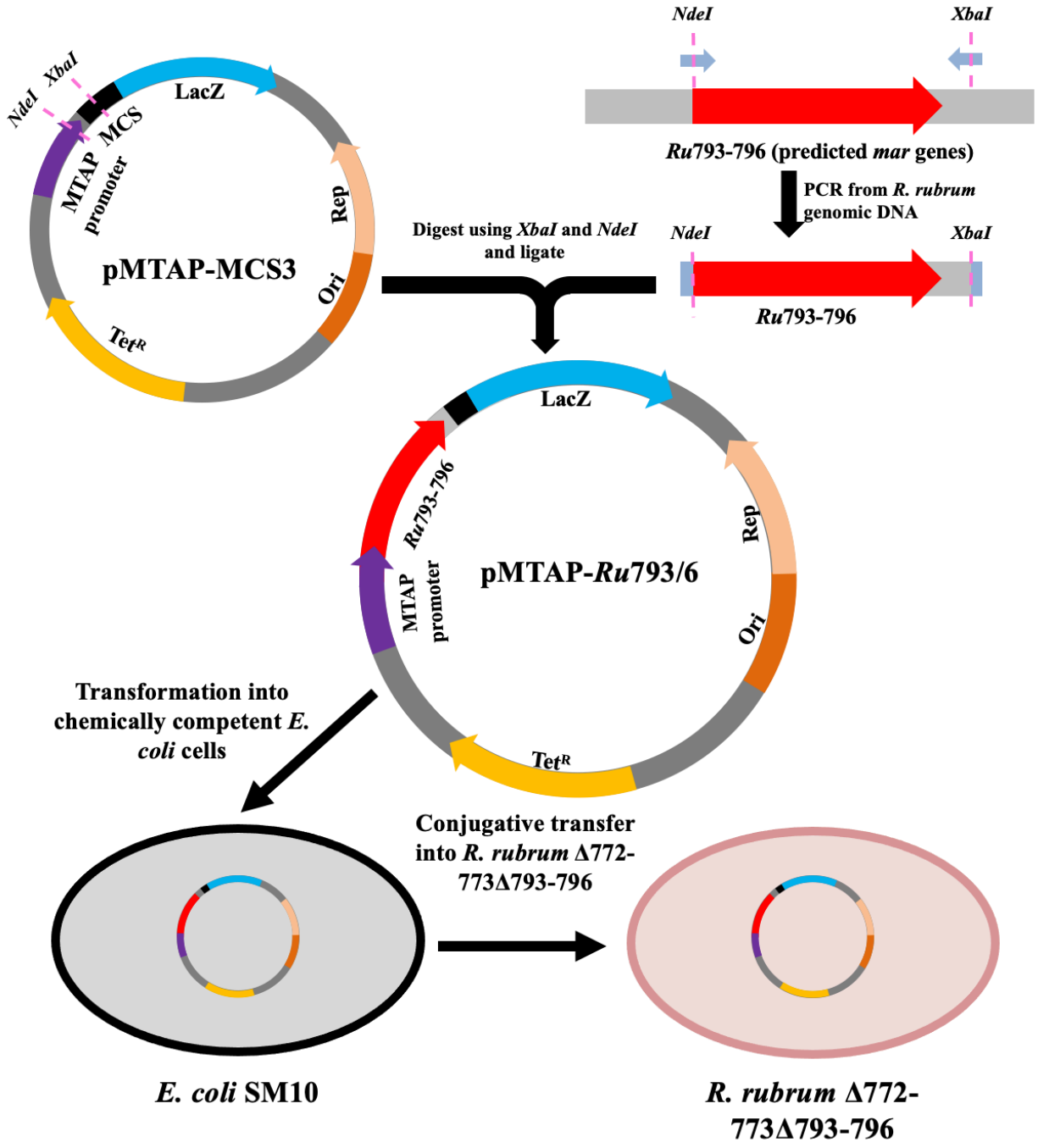

Figure 5: Schematic for construction of *R. rubrum* complementation strains. The genes of interest (represented above as Rru_A0793-Rru_A0796) were amplified by PCR, digested, and ligated into pMTAP-MCS3 plasmids. *E. coli* SM10 cells were then transformed with the pMTAP plasmids and mobilized into *R. rubrum* Δ0772:3/Δ0793:6 via conjugative transfer.

Primer Description	Primer Name	Fragment Number	Sequence (5' – 3')	Fragment R.E.*	Plasmid R.E.†
Construction of pK18-Ru0793:6 from pK18mobsacBgm	R0793F	1	CTGTTTCAGGATCCTGGGTCCGCGGTACTCTATC	*BamHI*	*BamHI*
	R0793R	1	CCTGACTTTTCTAGAAAAAATCTACACAACCACCGTCAGCG	*XbaI*	--
	R0796F	2	GAAACTCCGACTAGTGCAGGCTGGCGGGAAGGATAAGC	*SpeI*	--
	R0796R	2	GCGCAAGGGCATGCCGTTGTCCATCGTGTATGGCG	*SphI*	*SphI*
Construction of pK18-Ru0772:3 from pK18mobsacBgm	R0772F	1	CAAAGGTGGATCCACAACGCCACTTTATCCTCCGC	*BamHI*	*BamHI*
	R0772R	1	CGGCTGTTTCTAGACGCCATCACCCACAAACTCCAG	*XbaI*	--
	R0773F	2	CGTCGTTCGACTAGTTCGACCGGCTGGAGCGGC	*SpeI*	--
	R0773R	2	CCGTATCGGCATGCATGCCAACCCAGGACGCCTTTG	*SphI*	*SphI*
Construction of pMTAP-Ru0795:6 from pMTAP-MCS3	C0796F	1	GGAGACGGCTCATATGACGGTTCCTGCTTATCCTTCCCGC	*NdeI*	*NdeI*
	C0795R	1	GATGGGCATGGTACCCGTTATGAGGCCAGG	*KpnI*	*KpnI*
Construction of pMTAP-Ru0793:4 from pMTAP-MCS3	C0794F1	1	CGGAGCGGCCATATGCCCATCAATCTCAAGACATCGGTGG	*NdeI*	*NdeI*
	C0793R	1	GGCGGCCTCGAGCCCGGATGCCGCCATTCC	*XhoI*	*XhoI*
Construction of pMTAP-Ru0793:6 from pMTAP-Ru0795:6	C0794F2	1	CGGAGCGGTACCATGCCCATCAATCTCAAGACATCGG	*KpnI*	*KpnI*
	C0793R	1	GGCGGCCTCGAGCCCGGATGCCGCCATTCC	*XhoI*	*XhoI*
Construction of pMTAP-Ru0795:6/Ru0772:3 from pMTAP-Ru0795:6	C0773F	1	GGAGGCGGGTACCGTGACAAAGATCGAAAAGCCGCTCCAGCC	*KpnI*	*KpnI*
	C0772R	1	CATCACCCCTCGAGCCACACCGGGCGACCGCACAGC	*XhoI*	*XhoI*

Table 1: Primers used in Chapter I methods. * Restriction enzymes were used to digest the indicated PCR amplicons (underlined sequence). † Restriction enzymes were used to digest the plasmid for incorporation of digested PCR amplicons by ligation.

Chapter I Results

All *R. rubrum* strains tested are able to grow on 1 mM ammonium sulfate as the sole sulfur source due to active sulfur assimilation of sulfate into cysteine and methionine[1]. This is because sulfur assimilation pathways do not require the DHAP—ethylene shunt. All other sulfur sources analyzed—1 mM MT-EtOH, 1 mM EMS, or 1 mM DMS—to serve as the sole sulfur source would, however, require metabolism to methionine via an alternate pathway. *R. rubrum* Δ0772:3 exhibited ability to grow on all sulfur sources but with an increased lag time compared to *R. rubrum* wild type (Figure 6). *R. rubrum* Δ0793:6 did not grow with any of the three volatile organic sulfur substrates (Figure 6). Therefore, a double deletion strain was made to test the various requirements of the Nfl genes, Rru_A0772- Rru_A0773 and Rru_A0793-Rru_A0796, for the anaerobic ethylene pathway. *R. rubrum* Δ0772:3/Δ0793:6 could not grow using the volatile organic sulfur substrates similarly to *R. rubrum* Δ0793:6 (Figure 6).

Phylogenetic comparisons of the Rru_A0772-Rru_A0773 and Rru_A0793-Rru_A0796 genes indicated they were nitrogenase-like genes (Table 2; original analysis performed by Dr. Justin North and our collaborators at Colorado State University). Thus, gene combinations selected for the complementation studies mixed the nitrogenase-like components between the two gene clusters. The inability of all combinations of the Nfl genes in the complementation studies to grow on the alternative sulfur sources of DMS or MT-EtOH (except for *R. rubrum* Δ0772:3/Δ0793:6 complemented with Rru_A0793-Rru_A0796), indicates those transgenic combinations were not sufficient for a functional pathway (Figure 7). The ability of only *R. rubrum* Δ0772:3/Δ0793:6 complemented with Rru_A0793-Rru_A0796 to successfully grow on 1 mM DMS, EMS, or MT-EtOH (Figure 7) indicates those four genes (Rru_A0793-Rru_A0796)

are required and sufficient to restore the anaerobic ethylene pathway and convert the provided sulfur source to methanethiol, the methionine precursor.

The identification of Rru_A0793-Rru_A0796 as the genes involved in anaerobic ethylene pathway was confirmed in the gas chromatography studies. Ethylene, ethane, and methane were each produced from MT-EtOH, EMS, or DMS substrates, respectively. The lack of ethylene, ethane, or methane production by the *R. rubrum* Δ0772:3/Δ0793:6 strain expressing other distinct gene combinations (Figure 9) further confirms that they do not restore the anaerobic ethylene pathway.

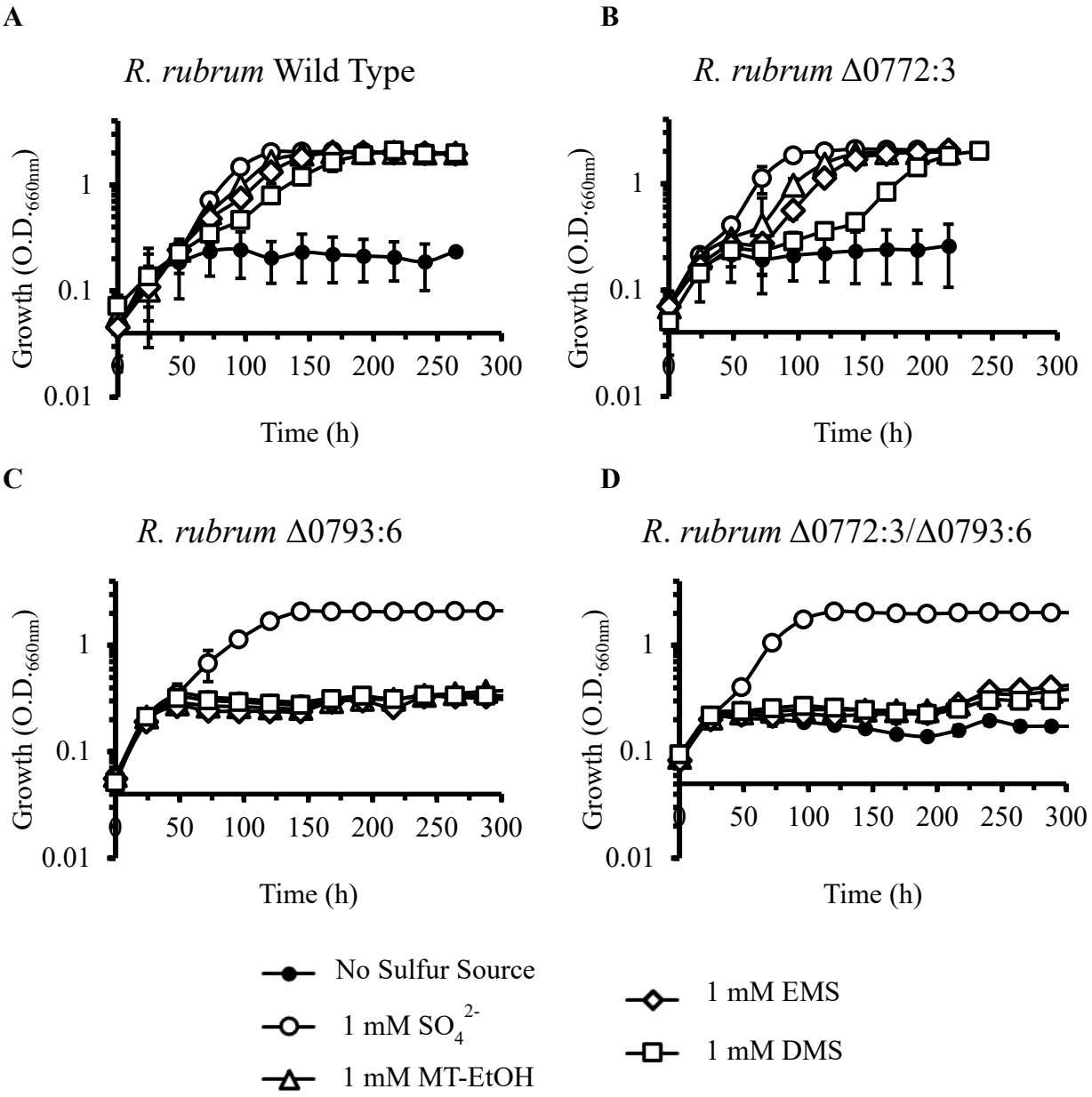

Figure 6: Growth studies of *R. rubrum* gene deletion strains with varying sulfur sources. Growth of *R. rubrum* Wild Type (A) as well *as R. rubrum* strains in which the gene clusters Rru_A0772-Rru_A0773 (B), Rru_A0793-Rru_A0796 (C), and Rru_A0772-Rru_A0773/Rru_A0793-Rru_A0796 (D) were deleted. Cultures were grown anaerobically in MMM supplemented with 1 mM of the indicated sulfur source (as indicated in legend) or no sulfur source.

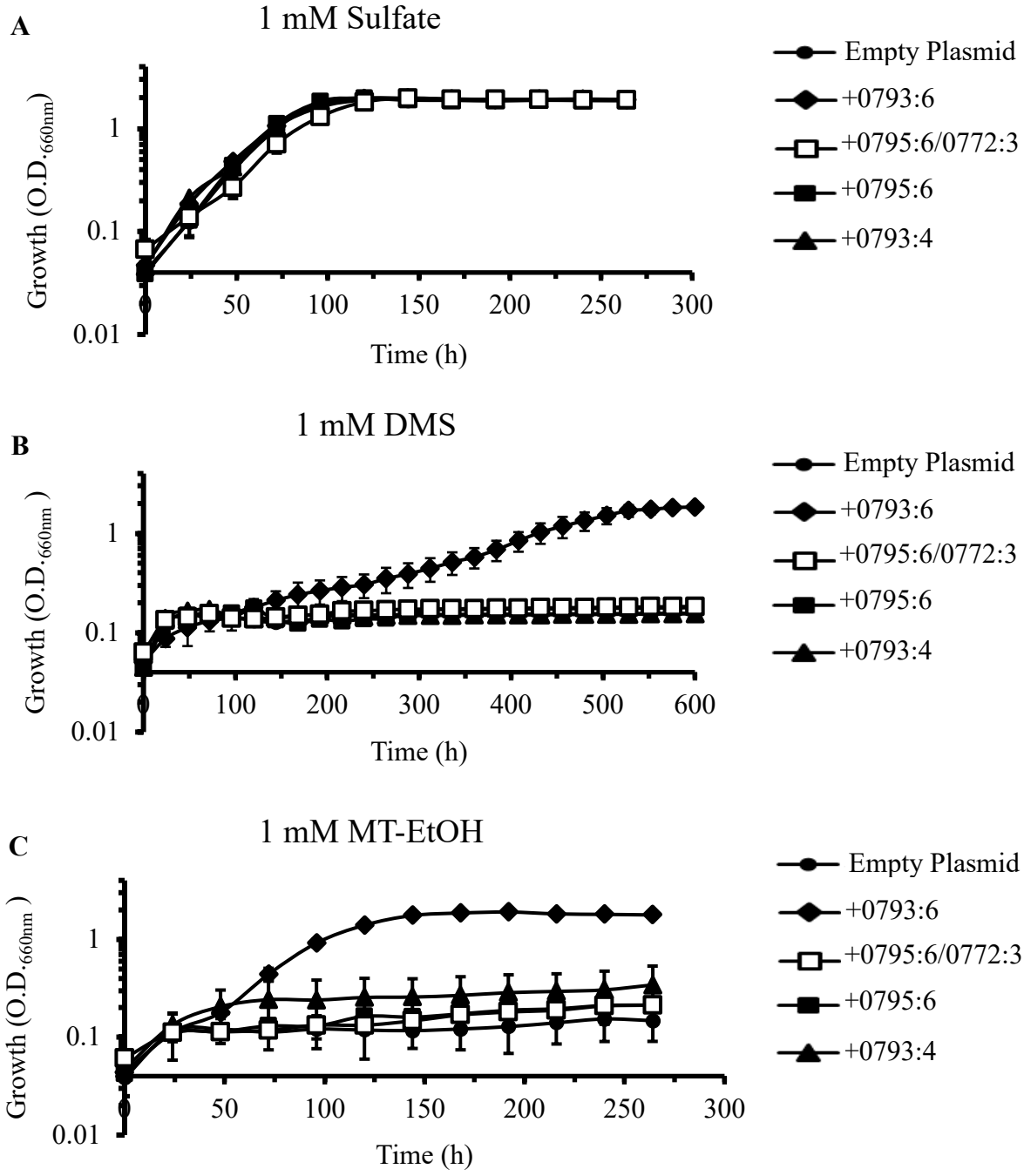

Figure 7: Growth studies of *R. rubrum* gene complementation strains. Growth of *R. rubrum* Δ0772:3/Δ0793:6 complemented with various nitrogenase-like gene combinations from *R. rubrum* (as indicated in legend). Cultures were grown anaerobically in MMM supplemented with 1 mM sulfate (A), 1 mM DMS (B), or 1 mM MT-EtOH (C).

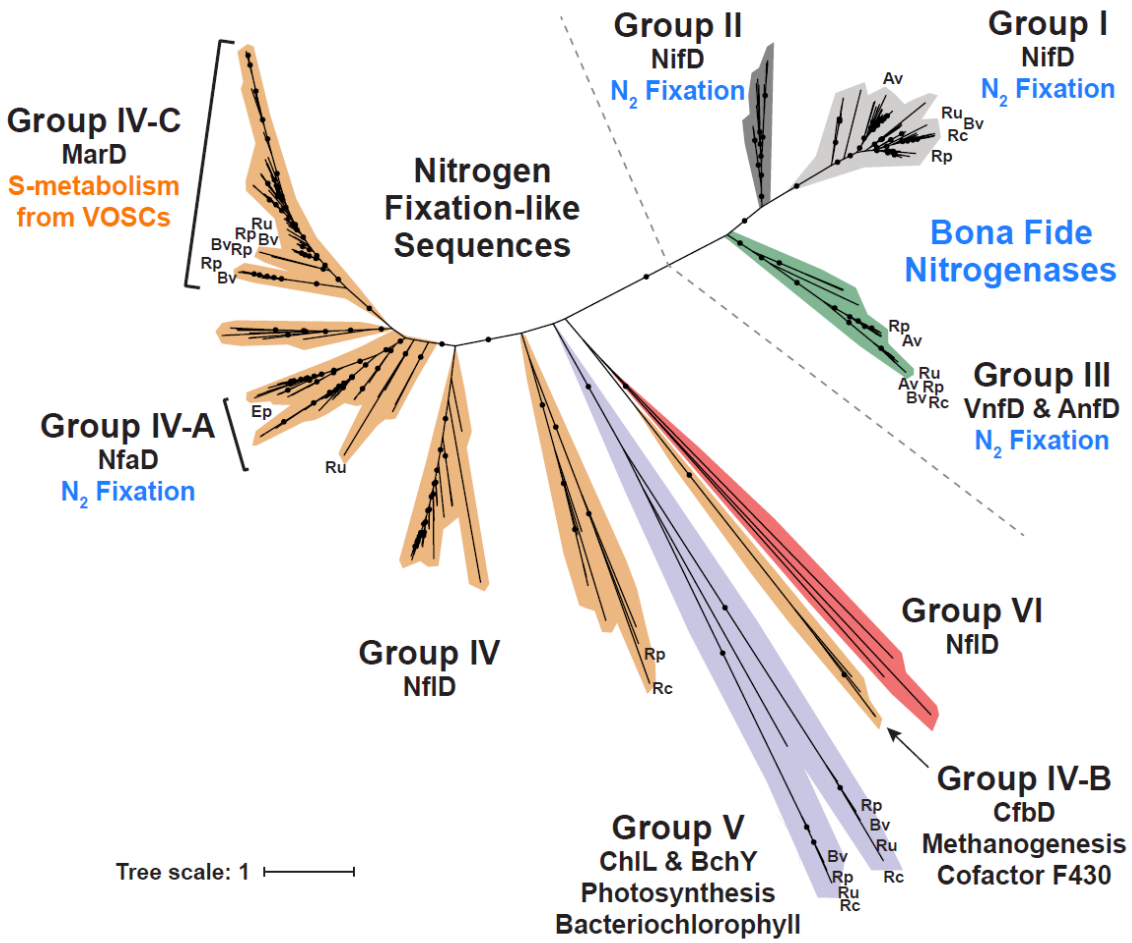

Figure 8: Amino acid phylogenetic analysis of nitrogenase subunit D sequences reproduced from North et al.[19], performed by Dr. Adrienne Narrowe. Phylogenetic tree of NifD superfamily homologues. The scale bar represents the number of amino acid substitutions per site. Nodes with UFBoot support values ≥ 95% are indicated with black circles. Clade labeling: Group IV-A (NfaD; nitrogen fixation IV-A), Group IV-B (CfbD; Ni2+-sirohydrochlorin a,c-diamide reductive cyclase), Group IV-C (MarD; putative methylthio-alkane reductase), Group IV and Group VI (NflD; nitrogen fixation-like of unknown function), Group V (ChlN; DPOR, and BchY; COR). Clade labels and colors are per Raymond and Méheust. Av, *Azotobacter vinelandii*; Bv, *Blastochloris viridis*; Ep, *Endomicrobium proavitum*; Rc, *Rhodobacter capsulatus*; Rp, *Rhodopseudomonas palustris*; Ru, *Rhodospirillum rubrum*.

Gene	Conserved Residues in Nitrogenase Subunit Homologs that are Conserved in Anaerobic Ethylene Pathway Gene	Conserved Residues in Nitrogenase Subunit Homologs that are Not Conserved in Anaerobic Ethylene Pathway Gene
Rru_A0793 (MarK)	• Triad of cysteines (Cys-70, Cys-95, Cys-153) involved in P-cluster coordination	• No non-conserved residues observed associated with major, known functions
Rru_A0794 (MarD)	• Triad of cysteines (Cys-62, Cys-88, Cys-154) involved in P-cluster coordination • Cysteine (Cys-275) for FeMo-cofactor coordination	• Histidine (His-442) for FeMo-cofactor coordination • Glutamate (Glu-191) and histidine (His-195) for substrate coordination for interaction with FeMo-cofactor
Rru_A0795 (MarH)	• Residues (9-16) for MgATP binding • Cysteines (Cys-97, Cys-132) for Fe_4-S_4 coordination • Arginine (Arg-100) residue that undergoes post-translational modification to regulate complex activity	• No non-conserved residues observed associated with major, known functions
Rru_A0796 (MarB)	• Radical SAM triad of cysteines (Cys-67, Cys-71, Cys-74) for Fe_4-S_4 coordination for eventual cofactor formation	• No non-conserved residues observed associated with major, known functions

Table 2: Results from Nif superfamily amino acid alignments using Rru_A0793-Rru_A0796, original analysis performed by Dr. Justin North[19]. Results of the comparison of Rru_A0793-Rru_A0796 (MarBHDK) to NifBHDK superfamily sequences from pairwise alignment analysis. Numbering is based off of *Azotobacter vinelandii*. Indicated associated function is for residues in bona fide nitrogenases.

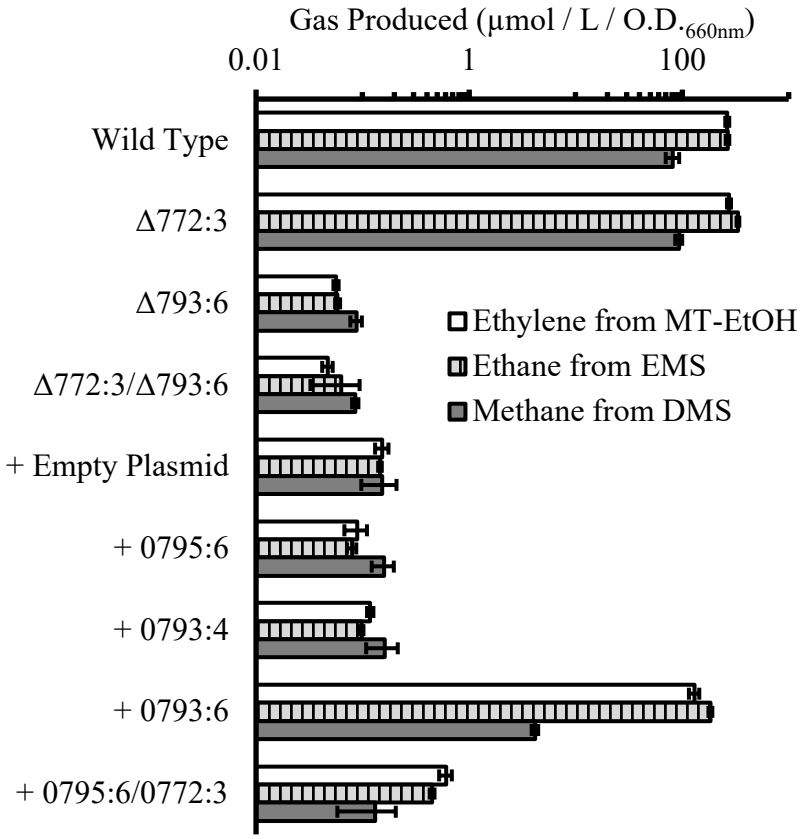

Figure 9: Gas production by *R. rubrum* gene complementation strains. Gas (ethylene, ethane, or methane) produced in micromole per liter of culture per culture optical density at 660 nm (µmol / L / O.D.$_{660nm}$), on a logarithmic scale, by *R. rubrum* deletion strains complemented with various nitrogenase-like gene combinations from *R. rubrum*. Cultures were grown anaerobically in MMM supplemented with 1 mM DMS, 1 mM EMS, or 1 mM MT-EtOH.

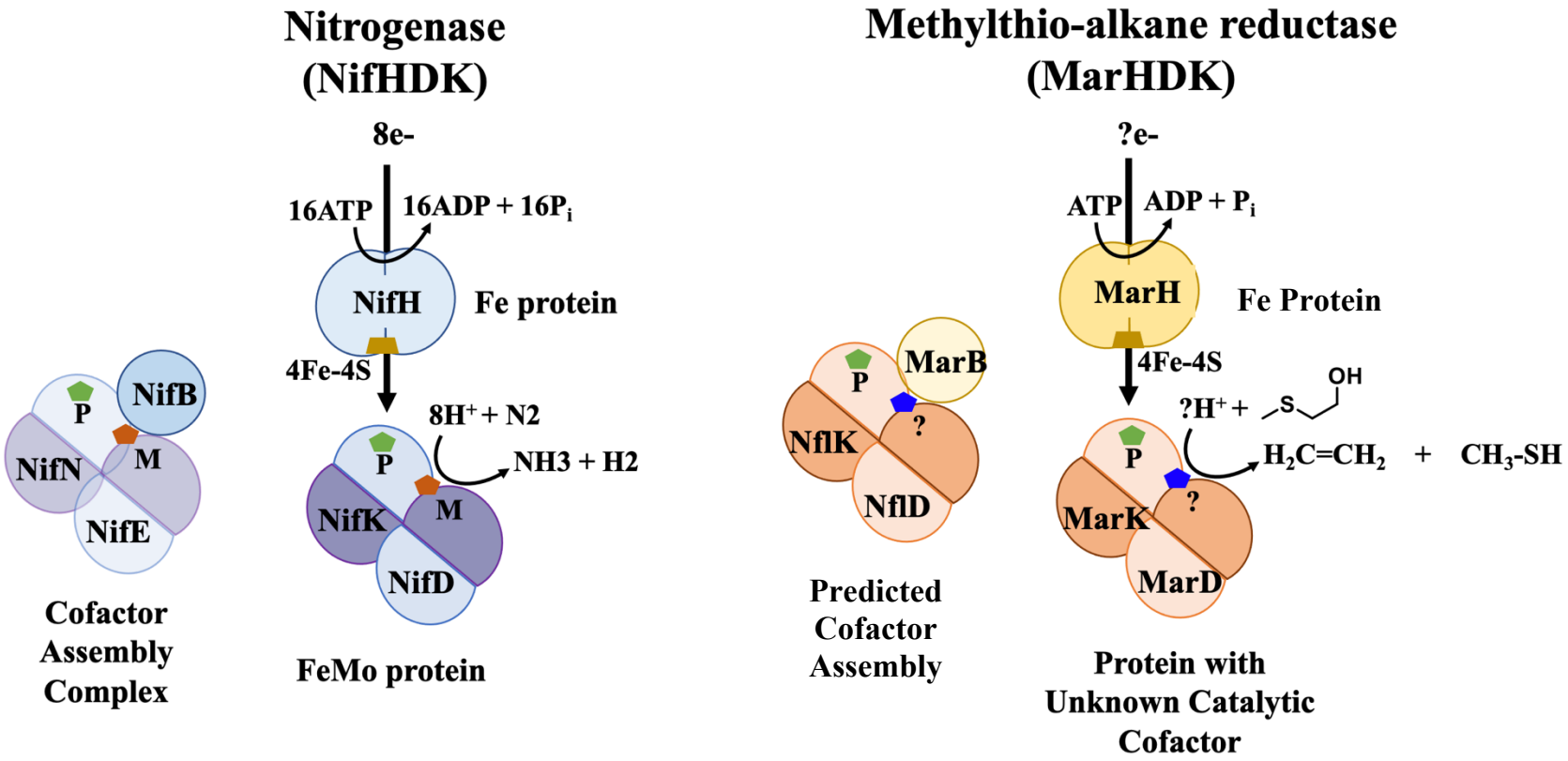

Figure 10: Pictorial representation of predicted MarHDK structured similarity to NifHDK. Based on phylogenetic comparisons of Rru_A0793-Rru_A0796, their corresponding gene products are distantly related homologs to the nitrogenase complex[19]. This relatedness indicates the structure and function of the putative MarHDK complex. "P" and "M" and the corresponding pentagons refer to the iron-sulfur clusters that act as electron carriers in nitrogenases. The blue pentagon represents the unknown additional cofactor corresponding to the MarHDK complex. NifHDK are the catalytic subunits of nitrogenases. NifB participates in formation and insertion of the cofactor into the catalytic nitrogenase subunits. NifEN participate in cofactor maturation of nitrogenases.

Chapter I Discussion

The results of the gene deletion and complementation studies indicate the genes Rru_A0793-Rru_A0796 are necessary and sufficient to restore the anaerobic ethylene pathway in strain *R. rubrum* Δ0772:3/Δ0793:6. The ability of the corresponding gene products to convert MT-EtOH, EMS, and DMS, to ethylene, ethane, and methane respectively indicates they constitute a promiscuous methylthio-alkane reductase. This is further supported by the observation methanethiol, a precursor to methionine, is a common product for each of these processes[19]. Phylogenetic comparisons revealed this gene cluster (acting as a methylthio-alkane reductase) is distantly related to nitrogenase (Table 2). Specifically, *R rubrum* genes Rru_A0796, Rru_A0795, Rru_A0794, and Rru_A0793 were designated as methylthio-alkane reductase *marB*, *marH*, *marD*, and *marK* based on amino acid homology with the products of nitrogenase *nifB*, *nifH*, *nifD*, and *nifK*, respectively. Thus, the nitrogenase-like methylthio-alkane reductase proteins are designated MarBHDK.

Analysis of Rru_A0772-Rru_A0773 revealed relatedness of their gene products to nitrogenase NifD and NifK subunits, respectively, but were located in a separate phylogenetically distinct clade separate from MarD and MarK (Figure 8). Thus, they were termed nitrogenase fixation-like (Nfl) DK. The homology between NflDK and MarDK could potentially explain the elevated production of ethylene in the gas chromatography studies of *R. rubrum* Δ0772:3/Δ0793:6 complemented with Rru_A0795-Rru_A0796/Rru_A0772-Rru_A0773 compared to the empty plasmid when grown on MT-EtOH (Figure 9). Since the complement did not fully restore function of the DHAP—ethylene pathway and the pathway remained active in *R. rubrum* Δ0772:3 (Figure 9), however, the primary function of NflDK remains unknown and will be a target of future studies.

The correspondence of MarBHDK to a nitrogenase-like enzyme complex indicates the nitrogenase superfamily catalyzes three essential elements. Bona fide nitrogenase enzyme complexes perform the majority of biological nitrogen fixation in nitrogen metabolism via reduction of dinitrogen gas into ammonia[11]. It has also been previously established that phylogenetically distinct nitrogenase fixation-like enzyme complexes are involved in carbon metabolism via functions in photosynthesis and archaeal methanogenesis cofactor synthesis (Figure 8 groups IV-B and V)[3,11,19]. The above experiments, however, indicate that distinct nitrogenase fixation-like enzyme systems like methylthio-alkane reductase are involved in sulfur metabolism (Figure 8 group IV-C).

The relatedness of MarBHDK to NifBHDK also has implications for how MarBHDK may function in the anaerobic ethylene pathway (pictorial comparison in Figure 10). Bona fide nitrogenases operate in reduction reactions via highly modified iron-sulfur metal clusters (including the P-cluster and M-cluster), which aid in the transfer of electrons[10]. The NifH nitrogenase subunit forms a homodimer in which it binds a single Fe_4-S_4 iron-sulfur cluster[10,19]. NifH transfers elections from the Fe_4-S_4 iron-sulfur cluster in an ATP-dependent fashion to NifDK[19]. The NifD and NifK nitrogenase subunits forms a heterotetramer that contains a P-cluster and a FeMo-cofactor at the two NifDK interfaces[10,19]. The P-cluster accepts the electrons being transferred by NifH. Importantly, the FeMo-cofactor [Fe_7-S_9-C-Mo-homocitrate] is the catalytic metal cofactor, which performs the ultimate transfer of electrons to the substrate[10,19]. The NifB subunit is a radical SAM enzyme which, in conjunction with NifEN, aids in forming and inserting the FeMo-cofactor into NifDK[7,19].

According to pairwise alignment analysis, MarH contains the same conserved residues as NifH for MgATP and iron-sulfur coordination that allows for the transfer of electrons from the

Fe_4-S_4 cluster associated with NifH to the NifDK P-cluster[10,19] (Table 2). This finding implies MarH may function similarly in the reduction of MarDK. MarH also has a conserved Arg-100 residue present in NifH (Table 2). Notably, this arginine residue regulates nitrogenase activity via post-translational modification. Arg-100 undergoes ADP-ribosylation which prevents interactions between NifH and the NifDK heterotetramer[8,19]. In *R. rubrum*, ADP-ribosylation of nitrogenases is performed by dinitrogenase reductase ADP-ribosyltransferase (DraT) and the modification is removed by dinitrogenase reductase activating glycohydrolase (DraG)[8,19]. The conserved Arg-100 in MarH suggests a similar regulation of MarBHDK activity may occur.

According to the pairwise alignment of MarD and MarK, MarDK each contain a conserved triad of cysteines present in NifDK that act in P-cluster coordination[4,19] (Table 2). MarD also has a conserved cysteine (Cys-275 using *A. vinelandii* numbering) which is used to coordinate the FeMo-cofactor in NifD[9,14,19] (Table 2). This finding suggests similar activity by MarDK compared to NifDK. The NifD His-442 residue used to coordinate the FeMo-cofactor homocitrate and molybdenum[9,19], however, is not conserved in MarD. Additional residues associated with coordinating the FeMo-cofactor are also not conserved in MarD (Table 2) suggesting a different cofactor may be associated with the MarBHDK system. According to the pairwise alignment, MarB exhibits the same conserved residues as the majority of NifB subunits which performs cofactor assembly[7,19] (Table 2). Therefore, MarB is putatively involved in MarDK assembly.

Chapter II: Partial Isolation and Characterization of MarBHDK

Material and Figures reproduced with permission from:

North, J.A., Narrowe, A.B., Xiong, W., Byerly, K.M., Zhao, G., Young, S.J., Murali, S., Wildenthal, J.A., Cannon, W.R., Wrighton, K.C., Hettich, R L., Tabita, F.R. (2020) A nitogenase-like enzyme system catalyzes methionine, ethylene, and methane biogenesis. *Science, 369*(6507), 1094-1098. doi:10.1126/science.abb6310

Chapter II Introduction

Based on homology studies, the next goal of this study was to isolate and characterize the active Mar complex in order to elucidate its function and the exact reactions it performs. Better understanding the complex is critical for both engineering this pathway for industrial ethylene production as well as understanding its functionality in environmental and pathogenic bacteria in relation to human health.

The identification of the Mar system as a member of the nitrogenase superfamily has implications for its potential location in the cell. Proteins in the nitrogenase superfamily are not typically trans-membrane nor membrane-bound, but some nitrogenase-associated proteins are membrane-associated[22]. Therefore, preliminary experiments were performed to determine the cellular location of the Mar system in order to purify the presumptive complex from *R. rubrum*.

The relatedness of the Mar system to nitrogenases also has implications for the requirements for its function in the anaerobic ethylene pathway. Traditionally, nitrogenases use adenosine triphosphate (ATP) for catalysis[10,19]. They also require available electrons either chemically, through reduced nicotine adenine dinucleotide or dithionite, or enzymatically, through ferredoxin and ferredoxin reductase[10,19]. Lastly, nitrogenases with a conserved Arg-100 residue in the H subunit regulate their activity via post-translational modification[8,19]. NifH

undergoes ADP-ribosylation by DraT which prevents interactions between NifH subunit and the NifDK heterotetramer. The modification is removed by dinitrogenase reductase activating glycohydrolase (DraG) in *R. rubrum*[8,19]. Any of these components could be required for Mar complex activity. Therefore, preliminary experiments were performed to determine the basic requirements for Mar activity. Experiments were also performed in both the presence and absence of light to eliminate any possibility of ethylene synthesis from other known pathways in which ethylene is a byproduct[24].

Prior purification of nitrogenase systems has been accomplished by adding a polyhistidine-tag to a catalytic subunit and isolation via a metal-affinity chromatography[15]. In the nitrogenase complex, NifHDK are catalytic[11]. Therefore, isolation of the Mar complex could potentially be performed in this manner.

To better understand the function and exact reaction performed by the MarBHDK system, cell-free extract assays were performed using *R. rubrum* wild type and *R. rubrum* Δ0772:3/Δ0793:6 complemented with a plasmid expressing $MarBHD_{His8}K$. The complementation strain of *R. rubrum* was then also used to isolate MarD and any stably bound partners via metal-affinity column chromatography.

Chapter II Methods

Bacterial Growth

R. rubrum ATCC 11170 wild type strain (Sm^R; NC_007643.1; American Type Culture Collection) with the gene deletions Rru_A0772-Rru_A0773/Rru_A0793-Rru_A0796 (henceforth referred to as *R. rubrum* Δ0772:3/Δ0793:6) was the background in which the complementation for eventual isolation and analysis was performed. Anaerobic growth of *R. rubrum* was performed in static anaerobic culture tubes and serum bottles at 30°C with 2000 lux incandescent illumination. Anaerobic cultures were composed of sulfer-free Omerod's MMM (Appendix) supplemented with the indicated sulfur source under a 95:5 mixture of N_2:H_2 gaseous headspace. Culture density was analyzed at an optical density (O.D.) of 660 nm. All harvesting, cell-free extract assays, and column chromatography was performed anaerobically in a 95:5 mixture of N_2:H_2 gaseous environment.

Construction of *R. rubrum* Complemented with His8-tagged MarBHDK

A schematic representation of the plasmid-based complementation of *R. rubrum* Δ0772:3/Δ0793:6 with methylthio-alkane reductase genes is shown in Figure 5 in Chapter I.

i) Construction of pMTAP-Ru0793:4$_{His8}$/Ru0795:6 Plasmid

To construct the gene complemention strain, the pMTAP-Ru0795:6 plasmid from Chapter I was manipulated to additionally contain Rru_A0793-Rru_A0794 in which Rru_A0794 was modified to add a sequence that encoded a polyhistidine tag. This introduced a His_8-tag at the N-terminal end of MarD analogous to previous methods with NifD[18]. Primers were designed to flank either side of the Rru_A0793-Rru_A0794 gene cluster and to insert a restriction enzyme site for eventual ligation into the pMTAP-Ru0795:6 plasmid (Table 3). The primer flanking the Rru_A0794 also contained a sequence encoding a polyhistidine-tag. Rru_A0793-Rru_A0794$_{His8}$

was then amplified via PCR (appendix), digested with *KpnI* and *XhoI* using manufacturer's protocols (New England Biolabs), and purified using a QIAGEN PCR-cleanup kit following manufacturer's protocols. The pMTAP-Ru0795:6 plasmid was additionally digested with *KpnI* and *XhoI* using manufacturer's protocol (New England Biolabs), treated with Antarctic phosphatase (New England Biolabs) to decrease the likelihood of plasmid recircularization during ligation, and purified using a QIAGEN PCR-cleanup kit. The Rru_A0793-Rru_A0794$_{His8}$ gene cluster and pMTAP-Ru0795:6 plasmid were then ligated together using T4 DNA ligase (New England Biolabs) to form the pMTAP-Ru0793:4$_{His8}$/Ru0795:6 plasmid.

ii) **Transformation of *E. coli* with pMTAP-Ru0793:4$_{His8}$/Ru0795:6**

Chemically-competent *E. coli* SM10 cells[21] were transformed to contain pMTAP-Ru0793:4$_{His8}$/Ru0795:6. Five µL of ligation mixture was added to a 100 µL aliquot of chemically-competent *E. coli* SM10 cells and incubated on ice for 20 minutes. The mixture underwent a heat shock at 42°C for 1 minute and was incubated on ice again for an additional 5 minutes. Five hundred µL of SOC media (Appendix) was then added to the mixture and the culture was placed in a shaker table heated to 37°C for 1 hour. The cells were then spread-plated onto LB (Appendix)—1.6% (w/v) solid agar plates with 25 µg/mL kanamycin and 2 µg/mL tetracycline. Individual colonies were picked and grown in 5 mL of LB liquid media with 25 µg/mL kanamycin and 2 µg/mL tetracycline, and the plasmids were extracted using a QIAGEN Miniprep kit. Plasmid sequences were verified by sequencing at OSU-CCC Shared Resources, The Ohio State University.

iii) Conjugative Transfer of pMTAP-Ru0793:4$_{His8}$/Ru0795:6 into *R. rubrum*

The sequence-verified plasmid pMTAP-Ru0793:4$_{His8}$/Ru0795:6 was mobilized into *R. rubrum* Δ0772:3/Δ0793:6 by conjugative transfer using biparental mating with the transformed

E. coli SM10 cells. *R. rubrum* was initially grown aerobically at 30°C to late exponential phase in PYE (Appendix) liquid medium. *E. coli* SM10 transformants were grown aerobically at 37 °C to mid exponential phase in LB liquid medium. Strains were separately centrifuged and washed three times with PYE medium, combined in a 1:2 ratio of *E. coli* to *R. rubrum*, concentrated, and spotted onto a PYE—1.6% (w/v) solid agar plate. Biparental mating was carried out aerobically at 30°C for 2 days. *R. rubrum* transconjugants were selected on PYE—1.6% (w/v) solid agar plates with 2 μg/ml tetracycline and 50 μg/ml streptomycin under aerobic growth at 30°C.

Cell Growth and Harvesting

Using a starter inoculum of 6-7 mL of *R. rubrum* Δ0772:3/Δ0793:6 with pMTAP-Ru0793:4_{His8}/Ru0795:6 plasmid grown in an anerobic 15 mL culture, 165 mL cultures of the *R. rubrum* strain were grown anaerobically on MMM with 1 mM of EtOH to an $O.D._{660nm}$ of 1.3-1.6. The cultures were then harvested anaerobically, and two cultures were combined in a 500-mL anaerobic centrifuge bottle into which 300 μL of 1.7 M dithionite was added. The combined cultures were then centrifuged at 2,744 *g* for 15 minutes at 4°C in a JA10 rotor in a J21 Beckman Centrifuge. The supernatant was then discarded. This procedure and subsequent cell lysis for cell-free extract assays was additionally performed with the *R. rubrum* wild type strain.

Cell Lysis for Cell-Free Extract Assays

Three mL of lysis buffer (100 mM HEPES-KOH pH 7.4, 1 mM $MgCl_2$, 0.5 mM EDTA, 1 mM PMSF, 1 mM DTT, and 2 mM dithionite) per 100 mL of harvested culture was added anaerobically to the harvested pellet. The cells were resuspended and transferred to a chilled (-20 °C) French pressure cell. The attached outlet was a sealed serum vial ensuring the system was closed to oxygen. The cells were then lysed via the Sim Aminico SLM Instruments French Pressure Cell Press at 16,000 psi for one minute. The lysate was then transferred to a 50 mL

anaerobic centrifuge tube into which additional dithionite was added from a 1 M stock to achieve a 2 mM concentration. The lysate was then centrifuged on a JA20 rotor in the J21 Beckman Centrifuge at 17,640 *g* and 4°C for 20 minutes. The supernatant was separated and collected from the pellet.

Cell-Free Extract Assays

For the activity assays, components were added to a 5 mL anaerobic serum vial (resulting in a reaction volume of 2 mL and gaseous headspace of 3 mL). Ten µL of 2 mg/mL *R. rubrum* DraG was added to a final concentration of 0.05 mg/mL (methods for expression and isolation of *R. rubrum* DraG via expression from a plasmid in *E. coli* described below). Ten µL of 1 M dithionite was added to a final concentration of 2 mM. Five hundred µL of 4X concentration of ATP regeneration system (16 mM ATP, 20 mM $MgCl_2$, and 80 mM creatine phosphate made in 50 mM HEPES-KOH 7.4, purged with N_2 gas and stored at -20°C) was added to a final concentration of 1X. Four hundred µL of 50 mM HEPES-KOH was added to a final concentration of 10 mM. One mL of the supernatant or the membranes contained in the pellet resuspended in lysis buffer (described above in cell lysis for cell-free extract assay protocol) was then added. The reaction was initiated with 20 µL of 0.1 M MT-EtOH for a final concentration of 1 mM. Upon adding the substrate, the serum vial was immediately capped and incubated at 30°C in either the dark or under 2000 lux incandescent illumination. For manipulations of the included components, an equivalent volume of anaerobic water was added instead of the selected component. Production of ethylene was analyzed via gas chromatography 18 hours after initiating the reaction as described below.

Gas Chromatography Analysis

Quantification of ethylene was performed using a Shimazdu GC-14A with Restek Rt-Alumina BOND/Na_2SO_4 column. Gaseous culture headspace after cell-free extract assays as described above was injected (250 µL) at 180 °C and separated isothermally at 30°C with helium as the carrier gas. Eluted compounds were detected by flame ionization detector at 180 °C and identified based on retention time of methane and ethylene standard (Praxair). The total amount of each hydrocarbon present was calculated from the peak area as compared to standard concentration curves of the corresponding reference standard.

Expression and Purification of *R. rubrum* DraG

i) Construction of pET28-DraG Plasmid

To express *R. rubrum* DraG in *E. coli*, a pET28-DraG plasmid was made. Primers were designed to flank either side of the Rru_A1008 gene (which produces the DraG protein) and to insert a restriction enzyme site for eventual ligation into the pET28 plasmid (Table 3). Rru_A1008 was then amplified via PCR (appendix), digested with *NdeI* and *BamHI* using manufacturer's protocols (New England Biolabs), and purified using a QIAGEN PCR-cleanup kit. The pET28 plasmid was additionally digested with *NdeI* and *BamHI* using manufacturer's protocol (New England Biolabs), treated with Antarctic phosphatase (New England Biolabs) to reduce plasmid recircularization during ligation, and purified using a QIAGEN PCR-cleanup kit. The Rru_A1008 gene fragment and pET28 plasmid were then ligated together using T4 DNA ligase (New England Biolabs).

ii) Transformation of *E. coli* with pET28-DraG

Chemically-competent *E. coli* Rosetta DE3 pLysS cells (Millipore) were transformed to contain pET28-DraG. Five µL of ligation mixture was added to a 100 µL aliquot of chemically-competent *E. coli* Rosetta cells and incubated on ice for 20 minutes. The mixture then underwent

heat shock at 42°C for 1 minute and was incubated on ice again for an additional 5 minutes. Five hundred µL of SOC media was then added to the mixture and the culture was placed in a shaker table heated to 37°C for 1 hour. The cells were then spread-plated onto LB—1.6% (w/v) solid agar plates with 34 µg/mL chloramphenicol and 25 µg/mL kanamycin. Individual colonies were picked and grown in 5 mL of LB supplemented with 34 µg/mL chloramphenicol and 25 µg/mL kanamycin, and the plasmids were extracted using a QIAGEN Miniprep kit. Plasmid sequences were verified by sequencing at the OSU-CCC Shared Resources, The Ohio State University.

iii) *E. coli* Growth, Induction and Cell Harvest

E. coli pet28-DraG transformants were grown overnight aerobically at 18°C in 250 µM IPTG in LB liquid media. The culture was then chilled on ice for 10 minutes. The culture was transferred to a 500 mL centrifuge bottle and harvested via centrifugation at 2,744 *g* for 10 minutes at 4°C on a JA10 rotor in the J21 Beckman Centrifuge. The supernatant was discarded, and the pellet was washed once via resuspension in a cell wash buffer (50 mM MOPS pH 7.5, 300 mM NaCl, and 20% v/v glycerol) and re-pelleted via identical centrifugation conditions. Cells were resuspended in 1.4 mL per gram harvested cell pellet of native lysis buffer (50mM MOPS 7.5, 300mM NaCl, 20% v/v glycerol, and 10 mM imidazole) and supplemented with 1 mM DTT. The cells were lysed via the Sim Aminico SLM Instruments French Pressure Cell Press at 16,000 psi for one minute. The cell lysate was supplemented with 1 mM DTT, 1 mM PMSF, and 1 M additional NaCl to 750 mM final concentration of NaCl. Subcellular fractionation was carried out via centrifugation at 4°C for 20 min at 17,640 *g* to remove cell debris on a JA20 rotor in a J21 Beckman Centrifuge. The supernatant was the separated and diluted two-fold with the same cell wash buffer as described above.

iv) Purification of DraG from Cell Lysate

The supernatant from the cell lysate was then applied to a 5-mL Ni-NTA column (Qiagen) that was equilibrated with the same native lysis buffer as above. The column was washed with native lysis buffer followed by native wash buffer (50mM MOPS pH 7.5, 300 mM NaCl, 20% v/v glycerol, and 20 mM imidazole). DraG was eluted via washing the column with native elution buffer (50 mM MOPS pH 7.5, 300 mM NaCl, 20% v/v glycerol, and 250 mM imidazole). Fractions were analyzed by SDS-PAGE (procedure described below). DraG was then dialyzed into a storage buffer (50 mM MOPS pH 7.5, 300mM NaCl, 20% v/v glycerol, 1mM DTT, and 0.5mM $MnCl_2$) for use in the cell-free extract assays.

Cell Lysis for Purification of MarBHD$_{His8}$K

Three mL of lysis buffer (100 mM HEPES-NaOH pH 7.4, 300 mM NaCl, 20 mM imidazole, 0.5 mM EDTA, 1 mM PMSF, 1 mM DTT, and 2 mM dithionite) per 100 mL of harvested culture was added anaerobically to the harvested pellet from the *R. rubrum* Δ0772:3/Δ0793:6 with the pMTAP-Ru0793:4$_{His8}$/Ru0795:6 plasmid (described above). The cells were resuspended and transferred to a chilled (-20°C) French pressure cell. The attached outlet was a sealed serum vial ensuring the system was closed to oxygen. The cells were then lysed via the Sim Aminico SLM Instruments French Pressure Cell Press at 16,000 psi for one minute. The lysate was then transferred to a 50 mL anaerobic centrifuge tube into which additional dithionite was added from a 1 M stock to achieve a 2 mM concentration. The lysate was then centrifuged on a JA20 rotor in a J21 Beckman Centrifuge at 17,640 *g* at 4°C for 20 minutes. The supernatant was then separated and collected from the pellet. The supernatant was supplemented with an additional 2 mM of dithionite and MarD$_{His8}$ (with any stably bound partners) was isolated as described below.

Isolation of MarD$_{His8}$ and Stably-Bound Partners

The BioLogic Dual Flow (BioRad) fast performance liquid chromatography (FPLC) was used. A 5 mL column was packed with Ni-NTA agarose (Qiagen) and washed briefly with water. The packed column was then washed with five column volumes of equilibration buffer (0.025 M Tris pH 7.9, 0.5 M NaCl, and 2 mM dithionite). The cell lysate (as described above) was then applied to the column at approximately 0.3 L per hour. The column was washed with five column volumes of wash buffer (0.025 M Tris pH 7.9, 0.5 M NaCl, 20 mM of imidazole, and 2 mM dithionite). The protein was then eluted with elution buffer (0.025 M Tris pH 7.9, 0.5 M NaCl, 250 mM of imidazole, and 2 mM dithionite) and analyzed by SDS-PAGE.

Protein Analysis via Gel (SDS-Page) Electrophoresis

A 7% acrylamide stacking gel (Appendix) and 12% acrylamide resolving gel (Appendix) were used to resolve the DraG protein and MarBHD$_{His8}$K complex via gel electrophoresis. The gel electrophoresis rig was filled with 1X Tris-glycine SDS running buffer (3% w/v Tris, 14% w/v glycine, and 1% w/v SDS) and run at a constant amperage of 0.2 Amp during the stacking phase and 0.3 Amp during the resolving phase. SDS loading dye (4% w/v SDS, 0.1 M Tris pH 6.8, 20% v/v glycerol, 0.01% w/v bromophenol blue) was added in equal volume ratio to samples for visualization following gel electrophoresis. The ladder used was the Dual Color Prestained Protein Standard from BioRad. Ten µL of the ladder or sample were added to a lane for each run. After running the gel, Coomassie blue staining was performed. A destaining solution (50% v/v water, 40% v/v methanol, 10% v/v acetic acid) was made. 0.001% w/v Coomassie R250 was added to an aliquot of the destaining solution to make the stain solution. The gel was shaken in the stain solutions for 30 minutes and then shaken in the destaining solution for 30 minutes. The gel was then visualized using a visible transilluminator.

Primer Description	Primer Name	Fragment Number	Sequence (5' – 3')	Fragment R.E.*	Plasmid R.E.†
Construction of pMTAP-Ru0793:4$_{His8}$/Ru0795:6 from pMTAP-Ru0795:6	C0794F3His	1	GGAGCGGTACCATGCCCATCcatcaccatcatcaccatcaccatAATCTCAAGACATCGGTGGTCGAGAGCC	*KpnI*	*KpnI*
	C0793R	1	GGCGGCCTCGAGCCCGGATGCCGCCATTCC	*XhoI*	*XhoI*
Construction of pet28-DraG	DraGF	1	GGAGCGGCATATGACCGGCCCTTCCGTACACGAC	*NdeI*	*NdeI*
	DraGR	1	CATCGGCCATGGATCCGCGTCCTTGCAAAGGGAAGG	*BamHI*	*BamHI*

Table 3: Primers used in Chapter II methods. * Restriction enzymes were used to digest restriction site in PCR amplicons incorporated by the corresponding primer (underlined sequence). Lowercase letters in C0794F3His indicate the sequence that codes for the polyhistidine tag. † Restriction enzymes were used to digest plasmid for incorporation of digested PCR amplicons by ligation.

Chapter II Results

Following construction of pet28-DraG, transformation of *E. coli*, protein induction, cell harvesting, and DraG protein isolation via column chromatography, the SDS-PAGE analysis revealed an isolated protein consistent with DraG at 31.8 kD (Figure 11). Another band of an unknown, larger impurity—that probably corresponded to a contaminating species or a DraG dimer—copurified with DraG.

Following the cell-free extract assays and analysis via gas chromatography, it was observed ethylene was produced using the supernatant from the cell lysis for cell-free extract assay procedures and not the membranes (Figure 12 part A). The samples in which MT-EtOH were not added to the serum vial served as negative controls because MT-EtOH acts as the substrate for the anaerobic ethylene pathway. Therefore, the samples in which no MT-EtOH were added represent the amount of background ethylene present in the gaseous headspace. Thus, all subsequent cell-free extract assays (Figure 12 part B) were done exclusively using the supernatant from the cell lysis for cell-free extract assay procedures.

Further cell-free extract assays and analysis via gas chromatography elucidated requirements of the Mar system for methylthio-alkane reductase activity in the anaerobic ethylene pathway. Ethylene was not produced if either the ATP regeneration system, dithionite, or MT-EtOH (as the substrate) were not present in the serum vial (Figure 12 part B). The presence or absence of light was not observed to affect the amount of ethylene produced in the assays. The presence of DraG was not required for production of ethylene, and its absence surprisingly resulted in a slight increase of observed ethylene ($n = 1$; Figure 12 part B).

For partial purification of the nitrogenase complex, cells lysate containing synthesized MarB, MarH, $MarD_{His8}$, and MarK was applied to a Ni-NTA column. Unbound proteins were

washed away with a low imidazole wash buffer, and bound proteins were eluted with high imidazole elution buffer. Elution fractions were then analyzed by SDS-page for protein content. Two prominent bands consistent with $MarD_{His8}$ at 56.4 kDa and MarK at 50.8 kDa were identified. Prominent bands consistent with MarH at 31.1 kDa and MarB at 34.3 kDa were not observed on the SDS-page gel (Figure 13). Given the number of additional bands present, it could not be determined if MarB and MarH were absent or present at low abundance.

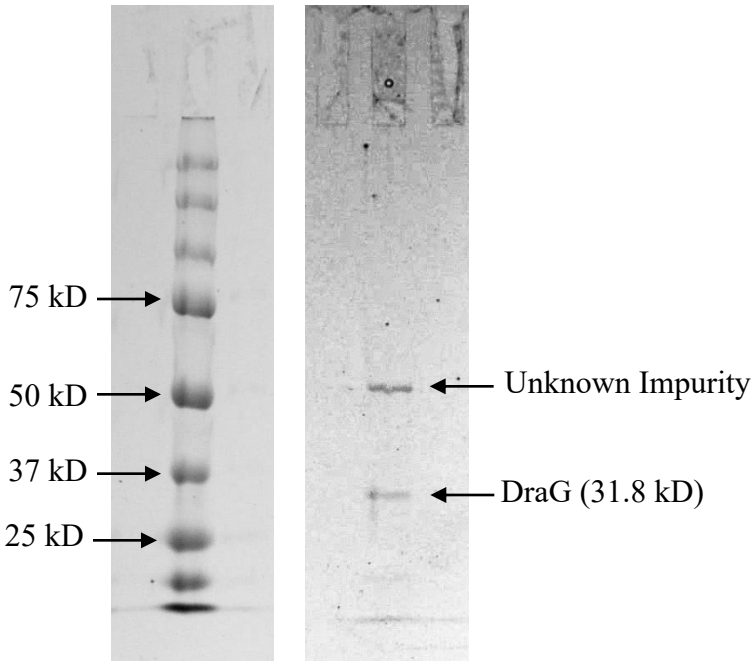

Figure 11: DraG protein isolation using metal affinity chromatography. Ten µL of ladder (BioRad Prestained Protein Standard Dual Color) was added to the first lane displayed on the left. Ten µL of DraG eluent was added to the lane on the right. Both lanes are splices from a photo of the same gel. The DraG protein has an expected mass of 31.8 kD.

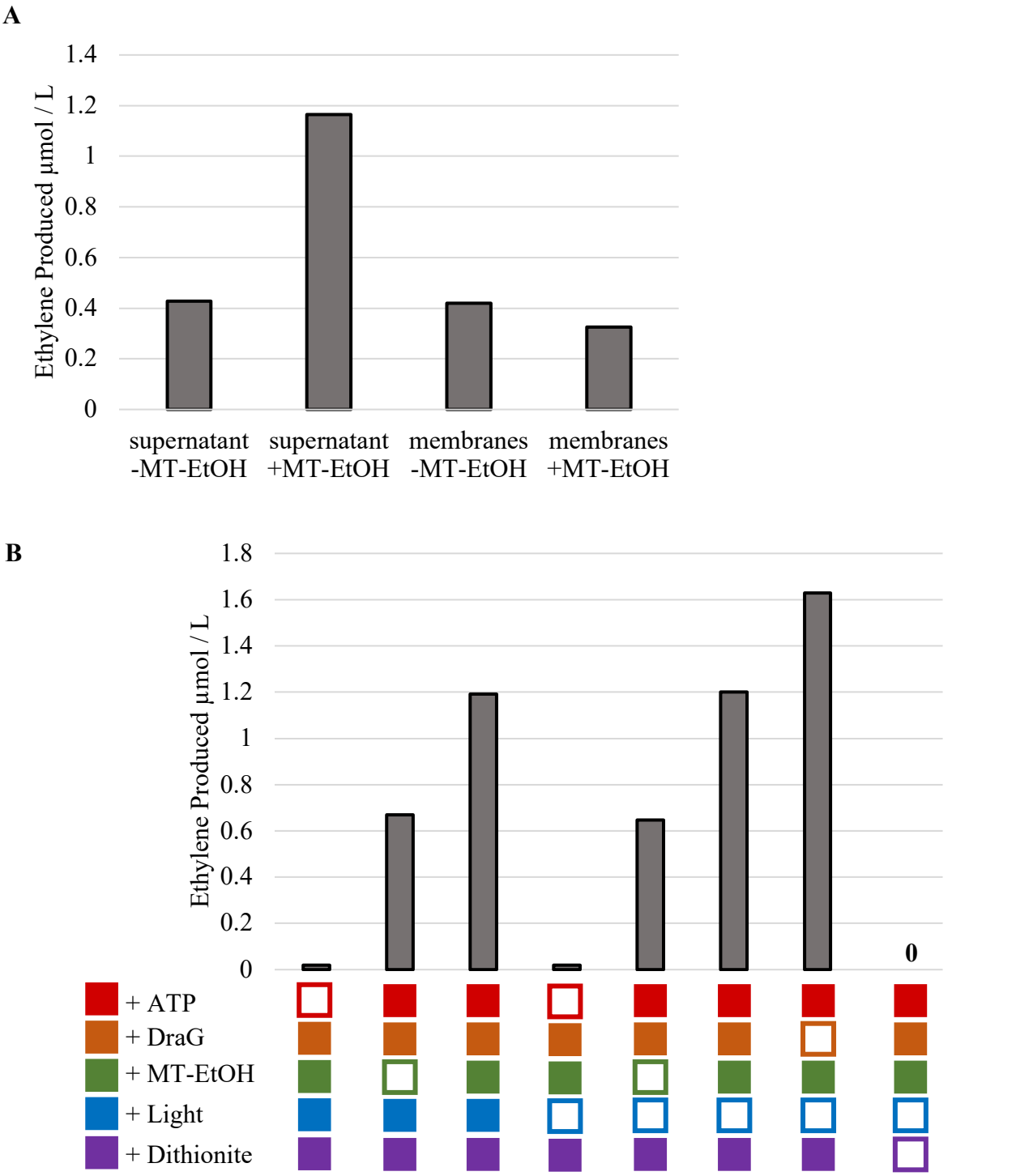

Figure 12: Ethylene production assays from *R. rubrum* cell-free extracts (n = 1). Ethylene production (µM) in *R. rubrum* wild type (A) and *R. rubrum* Δ0772:3/Δ0793:6 complemented with the pMTAP-Ru0793:4$_{His8}$/Ru0795:6 plasmid (B) in the cell-free extracts. Two hundred fifty µL of the gaseous headspace from the reaction serum vials were collected and analyzed via gas chromatography 18 hours after initiating the reaction with the substrate MT-EtOH. Solid shaded boxes designate the presence of the indicated component.

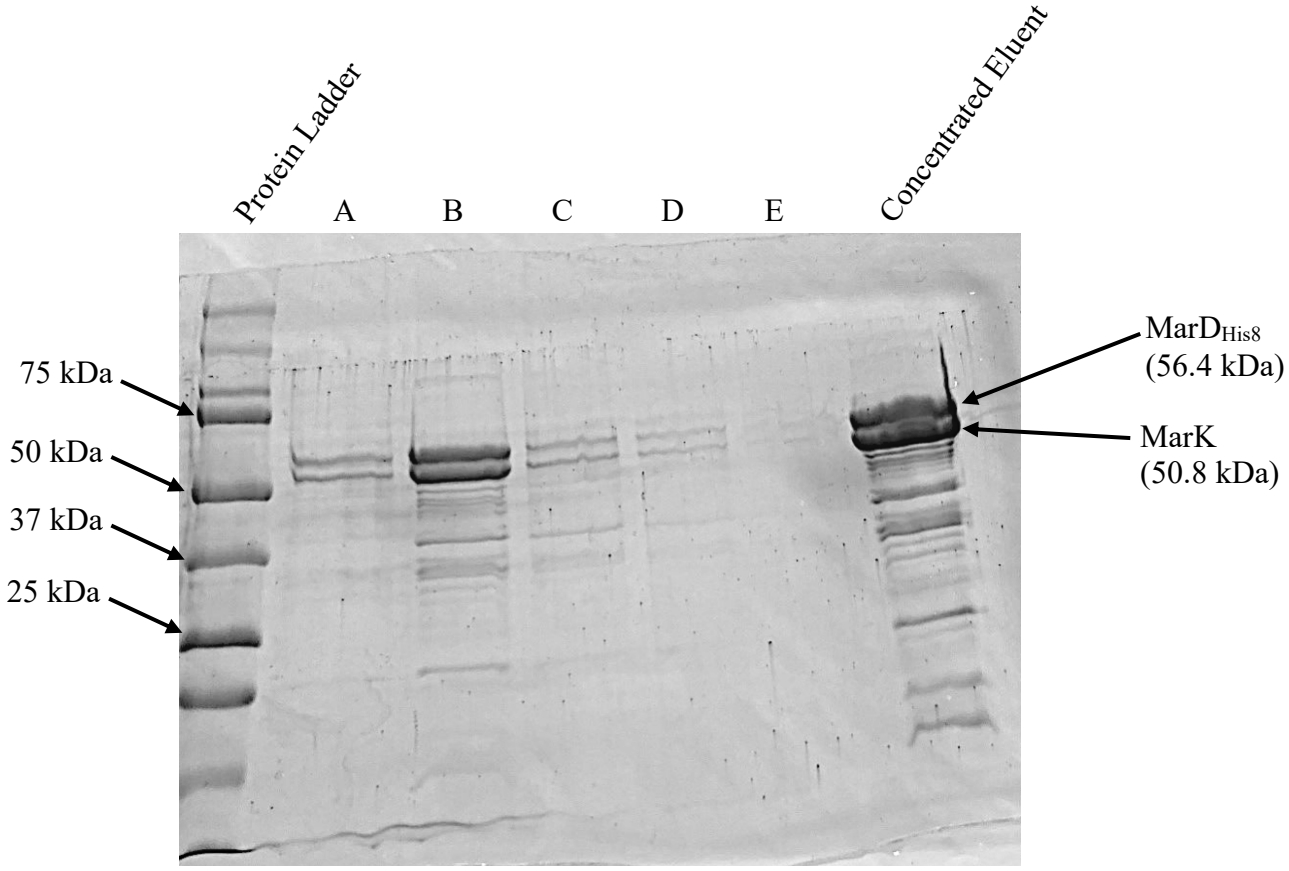

Figure 13: MarD protein isolation using metal affinity chromatography. Ten µL of ladder (BioRad Prestained Protein Standard Dual Color) was added to lane 1. Ten µL of five distinct fractions (A-E) from the column chromatography of lysed cells from *R. rubrum* Δ0772:3/Δ0793:6 complemented with the pMTAP-Ru0793:4$_{His8}$/Ru0795:6 plasmid were added to lanes 2-6. 10 µL of the concentrated eluent was applied to lane 7. The expected masses of the MarBHDK proteins are 34.3 kDa, 31.1 kDa, 56.4 kDa, and 50.8 kDa respectively.

Chapter II Discussion

The results of the cell-free extract assays indicated the Mar complex is located in the cytosol. The ethylene produced in the gas chromatography studies using the membranes isolated from *R. rubrum* wild type was the same for the reactions in which MT-EtOH (the substrate) was present or absent (Figure 12 part A). Therefore, there was no methylthio-alkane reductase present when using the insoluble membrane fraction. This implies the MarBHDK system, which is required based on the results of Chapter I for function of the anaerobic ethylene pathway, is soluble in the cytosol like other characterized proteins in the nitrogenase superfamily[22].

In the phylogenetics studies described in Chapter I, it was discovered the MarH subunit has a conserved Arg-100 which undergoes ADP-ribosylation in bona fide nitrogenases to prevent interactions between the NifH dimer and the NifDK heteotetramer[8,19] (Table 2). This post-translational modification in *R. rubrum* is performed by dinitrogenase reductase ADP-ribosyltransferase (DraT) and is removed (to allow activity) by dinitrogenase reductase activating glycohydrolase (DraG)[8,19]. The results of the cell-free extract assays indicated, however, the Mar complex is not regulated by DraG activity using the above methods and conditions. The ethylene produced by the extracts supplemented with the ATP regeneration system, dithionite, and MT-EtOH was actually higher when DraG was not present versus when it was (Figure 12 part B). If DraG did regulate the activity of the Mar complex, it would be required for functional activity of Mar in the DHAP—ethylene pathway and thus production of ethylene in the gas chromatography analysis of the cell-free extract assays (which is contradictory to the observed results).

One confounding factor, however, was the additional, unexpected band observed in the SDS-PAGE analysis of the purified DraG eluent (Figure 11). One possibility is that the band

corresponding to the unknown impurity corresponded to a DraG dimer, and would not interfere with Mar system activity. Another possibility is that the corresponding protein was an impurity that may have inhibited the activity of DraG or the Mar system. If the unknown impurity interfered with the activity of DraG, the increased ethylene observed in the absence of Drag during the cell-free extract assays (Figure 12 part B) would have been the product of a lack of replicates to identify difference significance via standard deviation. If the unknown impurity interfered with the activity of the Mar system, however, this would explain the increased ethylene observed in the absence of Drag during the cell-free extract assays (Figure 12 part B). The cell-free extract assays were performed to crudely determine the location of the Mar complex in the cell (membrane-bound versus soluble in the cytosol) and the basic requirements of the complex for function. Thus, the isolated solution containing DraG was not individually tested for activity and may not have been active. Therefore, future studies with the fully purified and active Mar system and DraG are required to confirm the involvement, or lack thereof, of DraG in regulating methylthio-alkane reductase activity.

The cell-free extract assays also indicated ATP is required for function of the Mar system in the anaerobic ethylene pathway. It was observed in the gas chromatography analysis for assays in which ATP regeneration system was not included that no ethylene was produced (Figure 12 part B). This indicates without ATP, the Mar system was not functional. In bona fide nitrogenases, ATP is required for catalysis[10,19]. The results of the cell-free extract assays suggest the Mar complex similarly requires ATP for catalysis.

The results of the cell-free extract assays indicated an available electron donor like dithionite is required for Mar system activity. The was no ethylene produced by the extract supplemented with the ATP regeneration system, the supernatant from the cell lysis for cell-free

extract assay procedures, DraG, and MT-EtOH, but no dithionite (Figure 12 part B). Bona fide nitrogenases require available electrons either enzymatically, via ferredoxin and ferredoxin reductase, or chemically, via dithionite or reduced nicotine adenine dinucleotide[10,19]. Therefore, the cell-free extract assays suggest the Mar system has the same requirement for activity.

Lastly, the cell-free extract assays indicated the presence or absence of light did not affect ethylene production (Figure 12 part B). This finding implies photochemistry was not involved in the function of the Mar complex or the production of the observed ethylene. This is significant because photochemistry can be used in an unrelated pathway in *R. rubrum* to produce low levels of ethylene (less than 0.1 μmol / L / $O.D._{660nm}$) from methionine[24] (pictorial representation of pathway demonstrated inn Figure 14). This generation occurs through a reaction in which flavin mononucleotide first undergoes photoreduction and then oxidizes methionine to methional which is converted immediately to ethylene[24]. Therefore, the same production of ethylene in both the presence and absence of light (Figure 12 part B) indicates the observed ethylene in the gas chromatography studies is a product of the anaerobic ethylene pathway and not the alternate pathway.

The results of the column chromatography purification of the MarD indicates the MarK subunit co-purifies with MarD, but MarH and MarB seemingly do not or at least at low levels (Figure 13). This finding implies the stable binding partner of MarD is MarK similar to NifD and NifK which form a heterotetramer in nitrogenases[10,19]. The number of additional bands observed on the gel, however, means the absence of MarB and MarH cannot be definitively ruled out. Future studies will be performed to determine if MarDK forms a heterodimer, heterotetramer, or a different type of complex possibly with the other subunits using gel filtration chromatography.

Prior isolation of nitrogenase complexes has been accomplished by adding a polyhistidine-tag to a catalytic subunit and recovery via a metal-affinity column[15]. Based on its relatedness to bona fide nitrogenase BHDK subunits, MarHDK are likely the catalytic subunits[11]. After a literature review, it was determined that a polyhistidine tag on the NifH subunit in bona fide nitrogenase complexes has not been historically successful[13]. Therefore, future studies will include expression and isolation of the MarH subunit via a plasmid recombinantly expressed in *E. coli*. The nitrogenase B subunit traditionally participates in cofactor assembly[7,19]. Therefore, future studies will also be required to determine if and how MarB is required for functional methylthio-alkane reductase assembly, activity, or both.

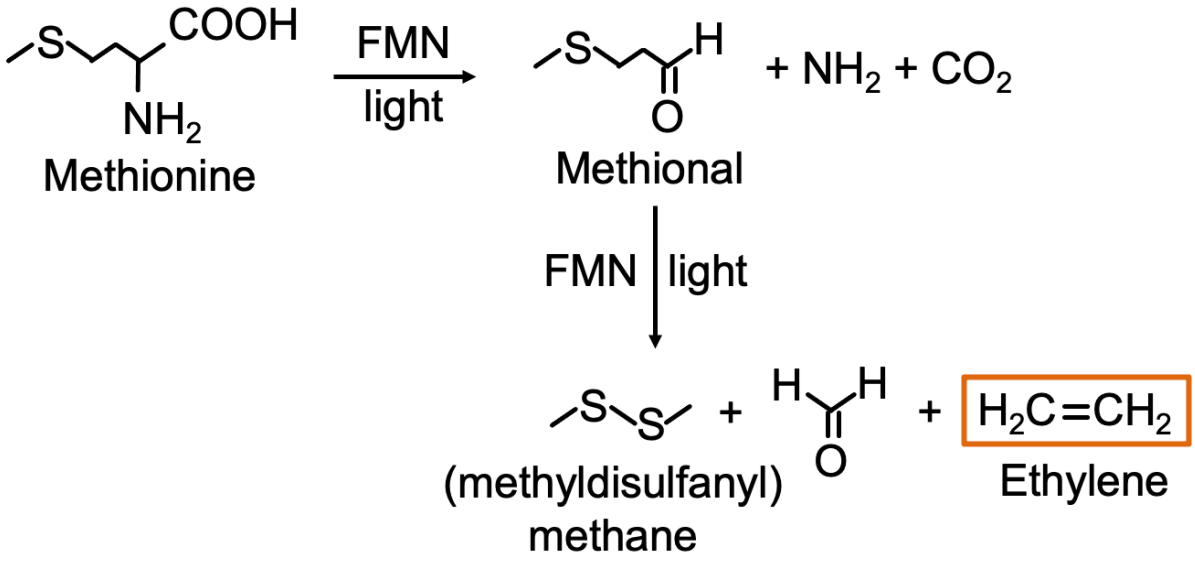

Figure 14: Pictorial representation of photochemical production of ethylene from methionine. When exposed to light, flavin mononucleotides (FMNs) undergo photoreduction and can participate in a pathway that produces ethylene. This pathway is distinct from the anaerobic ethylene pathway.

Future Directions

Future studies will work to fully characterize the DHAP—ethylene pathway and the activity of the methylthio-alkane reductase complex.

One subject of study will be the function of NflDK (Rru_A0772-Rru_A0773). NifDK in bona fide nitrogenases require NifEN, structural homologs of NifDK, for cofactor maturation[19]. Due to the close proximity of NflDK to MarDK and the homology of both NflDK and MarDK to NifEN and NifDK, respectively, NflDK may similarly function in assembly of the currently unknown cofactor of MarDK. This could potentially explain the partial restoration of methane production from the complementation studies in which *R. rubrum* Δ0772:3/Δ0793:6 complemented with Rru_A0793-Rru_A0796 (i.e. MarBHDK) exhibited less methane production when grown on DMS compared to *R. rubrum* wild type but full restoration of ethylene production when grown on MT-EtOH (Figure 13).

Another subject of study will be further analysis of the DraT / DraG as potential regulators of MarBHDK. DraT inactivates nitrogenases in *R. rubrum* via post-translational modification in which an ADP-ribosyl group is added to prevent interactions between the NifH homodimer and NifDK hetertetramer. DraG activates nitrogenases in *R. rubrum* by removing this ADP-ribosyl group[8,19]. The isolation protocol of DraG used in this study should be verified to determine if the DraG product is active. The impurity could also be isolated and analyzed via mass spectroscopy to determine if the unexpected band observed via SDS-PAGE was a DraG dimer or separate protein that also had affinity to the Nicked-NTA agarose resin. The confirmed active DraG protein and / or additional protein will then be tested with the purified Mar complex to confirm the involvement, or lack thereof, of DraG or the other impurity in the DHAP—ethylene pathway.

The last subject of future studies will be the full characterization of the purified Mar system. The purification process of MarD used in this study will be extended by running the concentrated protein recovered from the Nickel-NTA agarose resin over a gel filtration column. This will be used to eliminate the additional bands observed via SDS-PAGE analysis (Figure 13) and to determine if MarDK a heterodimer, heterotetramer, or a different type of complex possibly with the other subunits. Future studies will also include expression and isolation of the MarH subunit via recombinant expression from a plasmid in *E. coli*. The purified MarDK complex and MarH subunit (as the putative catalytic subunits) will then be combined to characterize the reaction the Mar complex performs. Lastly, future studies will also be performed to determine if and how MarB is required for Mar complex assembly, activity, or both.

References

1. Albers, E. (2009). Metabolic Characteristics and Importance of the Universal Methionine Salvage Pathway Recycling Methionine from 5'-methylthioadenosine. *IUBMB Life, 61*(12), 1132-1142. doi:10.1002/iub.278

2. Alshammari, A., Bagabas, A., Kalevaru, V. N., & Martin, A. (2016). Production of Ethylene and its Commercial Importance in the Global Market. In 1310745190 963669564 H. Al-Megren & 1310745191 963669564 T. Xiao (Authors), *Petrochemical Catalyst Materials, Processes, and Emerging Technologies* (pp. 82-115). Hershey, Pennsylvania: Engineering Science Reference. doi:10.4018/978-1-4666-9975-5.ch004

3. Blankenship R.E., Raymond J., Staples C., Mukhopadhyay B. (2008) Evolution of Functional Diversity in Nitrogenase Homologs. In: Dakora F.D., Chimphango S.B.M., Valentine A.J., Elmerich C., Newton W.E. (eds) Biological Nitrogen Fixation: Towards Poverty Alleviation through Sustainable Agriculture. *Current Plant Science and Biotechnology in Agriculture*, *42*, 305-306. doi:10.1007/978-1-4020-8252-8_119

4. Dean, D. R., Setterquist, R. A., Brigle, K. E., Scott, D. J., Laird, N. F., & Newton, W. E. (1990). Evidence that conserved residues Cys-62 and Cys-154 within the Azotobacter vinelandii nitrogenase MoFe protein alpha-subunit are essential for nitrogenase activity but conserved residues His-83 and Cys-88 are not. *Molecular Microbiology, 4*(9), 1505-1512. doi:10.1111/j.1365-2958.1990.tb02061.x

5. Dey, S., North, J. A., Sriram, J., Evans, B. S., & Tabita, F. R. (2015). In Vivo Studies in Rhodospirillum rubrum Indicate That Ribulose-1,5-bisphosphate Carboxylase/Oxygenase (Rubisco) Catalyzes Two Obligatorily Required and Physiologically Significant Reactions for Distinct Carbon and Sulfur Metabolic Pathways. *Journal of Biological Chemistry, 290*(52), 30658-30668. doi:10.1074/jbc.m115.691295

6. Erb, T. J., Evans, B. S., Cho, K., Warlick, B. P., Sriram, J., Wood, B. M., . . . Gerlt, J. A. (2012). A Rubisco-like Protein Links SAM Metabolism with Isoprenoid Biosynthesis. *Nature Chemical Biology, 8*(11), 926-932. doi:10.1038/nchembio.1087

7. Fajardo, A. S., Legrand, P., Payá-Tormo, L., Martin, L., Martínez, M. T., Echavarri-Erasun, C., . . . Nicolet, Y. (2020). Structural Insights into the Mechanism of the Radical SAM Carbide Synthase NifB, a Key Nitrogenase Cofactor Maturating Enzyme. *Journal of the American Chemical Society, 142*(25), 11006-11012. doi:10.1021/jacs.0c02243.s001

8. Fitzmaurice, W. P., Saari, L. L., Lowery, R. G., Ludden, P. W., & Roberts, G. P. (1989). Genes coding for the reversible ADP-ribosylation system of dinitrogenase reductase from Rhodospirillum rubrum. *Molecular and General Genetics, 218*(2), 340-347. doi:10.1007/bf00331287

9. Glazer, A. N., & Kechris, K. J. (2009). Conserved Amino Acid Sequence Features in the α Subunits of MoFe, VFe, and FeFe Nitrogenases. *Public Library of Science, 4*(7). doi:10.1371/journal.pone.0006136

10. Hoffman, B. M., Lukoyanov, D., Yang, Z., Dean, D. R., & Seefeldt, L. C. (2014). Mechanism of Nitrogen Fixation by Nitrogenase: The Next Stage. *Chem Rev, 114*(8), 4041-4062. doi:10.1021/cr400641x

11. Hu, Y., & Ribbe, M. W. (2015). Nitrogenase and homologs. *Journal of Biological Inorganic Chemistry, 20*(2), 435-445. doi:10.1007/s00775-014-1225-3

12. Iqbal, N., Khan, N. A., Ferrante, A., Trivellini, A., Francini, A., & Khan, M. I. (2017). Ethylene Role in Plant Growth, Development and Senescence: Interaction with Other Phytohormones. *Frontiers in Plant Science, 08*, 1-19. doi:10.3389/fpls.2017.00475

13. Jiménez-Vicente, E., Campo, J. S., Yang, Z., Cash, V. L., Dean, D. R., & Seefeldt, L. C. (2018). Chapter Nine - Application of affinity purification methods for analysis of the nitrogenase system from Azotobacter vinelandii. In 1260126734 932108928 F. Armstrong (Ed.), *Methods of Enzymology* (Vol. 613, pp. 231-255). doi:10.1016/bs.mie.2018.10.007

14. Kaluza, K., & Hennecke, H. (1984). Fine structure analysis of the nifDK operon encoding the α and β subunits of dinitrogenase from Rhizobium japonicum. *Molecular and General Genetics, 196*(1), 35-42. doi:10.1007/bf00334089

15. Lee, C., Ribbe, M. W., & Hu, Y. (2019). Purification of Nitrogenase Proteins. In *Metalloproteins: Methods and Protocols*(Vol. 1876). New York: Humana Press. doi:10.1007/978-1-4939-8864-8_7

16. Munk, A. C., Copeland, A., Lucas, S., Lapidus, A., Del Rio, T. G., Barry, K., Detter, J. C., Hammon, N., Israni, S., Pitluck, S., Brettin, T., Bruce, D., Han, C., Tapia, R., Gilna, P., Schmutz, J., Larimer, F., Land, M., Kyrpides, N. C., Mavromatis, K., … Schwartz, D. C. (2011). Complete genome sequence of Rhodospirillum rubrum type strain (S1). *Standards in genomic sciences*, *4*(3), 293–302. https://doi.org/10.4056/sigs.1804360

17. Parveen, N., & Cornell, K. A. (2011). Methylthioadenosine/S-adenosylhomocysteine nucleosidase, a critical enzyme for bacterial metabolism. *Molecular microbiology*, *79*(1), 7–20. https://doi.org/10.1111/j.1365-2958.2010.07455.x

18. North, J. A., Miller, A. R., Wildenthal, J. A., Young, S. J., & Tabita, F. R. (2017). Microbial pathway for anaerobic 5′-methylthioadenosine metabolism coupled to ethylene formation. *Proc Natl Acad Sci,114*(48), E10455-E10464. doi:10.1073/pnas.1711625114

19. North, J. A., Narrowe, A. B., Xiong, W., Byerly, K. M., Zhao, G., Young, S. J., . . . Tabita, F. R. (2020). A nitogenase-like enzyme system catalyzes methionine, ethylene, and methane biogenesis. *Science, 369*(6507), 1094-1098. doi:10.1126/science.abb6310

20. North, J. A., Wildenthal, J. A., Erb, T. J., Evans, B. S., Byerly, K. M., Gerlt, J. A., & Tabita, F. R. (2020). A bifunctional salvage pathway for two distinct S-adenosylmethionine by-products that is widespread in bacteria, including pathogenic Escherichia coli. *Molecular Microbiology, 113*(5), 923-937. doi:10.1111/mmi.14459

21. Simon, R., Priefer, U., & Pühler, A. (1983). A Broad Host Range Mobilization System for In Vivo Genetic Engineering: Transposon Mutagenesis in Gram Negative Bacteria. *Bio/Technology, 1*(9), 784-791. doi:10.1038/nbt1183-784

22. Smith, B. E., Campbell, F., Eady, R. R., Eldridge, M., Ford, C. M., Hill, S., . . . Yates, M. G. (1987). Biochemistry of Nitrogenase and the Physiology of Related Metabolism. *Philosophical Transactions of the Royal Society of London. B, Biological Sciences, 317*(1184), 131-146. doi:10.1098/rstb.1987.0052

23. Smith, K. A., & Russel, R. S. (1969). Occurrence of Ethylene, and its Significance, in Anaerobic Soil. *Nature,222*(5195), 769-771. doi:10.1038/222769b0

24. Yang, S., Ku, H., & Pratt, H. (1967). Photochemical Production of Ethylene from Methionine and Its Analogues in the Presence of Flavin Mononucleotide. *Journal of Biological Chemistry, 242*(22), 5274-5280. doi:10.1016/s0021-9258(18)99422-6

Appendix

1000X Sulfate-free Trace Elements
0.273% w/v $NiCl_2•H_2O$
0.247% w/v $MnCl_2•4H_2O$
0.28% w/v H_3BO_3
0.0273% w/v $CuCl_2$
0.074% w/v $NaMoO_4$
0.0247% w/v $CoCl_2$
0.306% w/v $Mn(CH_3CO_2)_2•4H_2O$

10X Sulfate-free Basal Salts
1.11% w/v KCl
0.203% w/v $MgCl_2$
0.0735% w/v $CaCl_2$
0.0068% w/v $FeCl_3$
0.0077% w/v $Zn(CH_3CO_2)_2•\ 2H_2O$
0.135% v/v EDTA •2 Na•$2H_2O$
1% v/v 1000X Sulfate-free Trace Elements

Vitamin Solution
0.1% w/v thiamin HCl
0.1% w/v nicotinic acid
50% v/v ethanol
50% v/v water

Biotin Solution
10 % w/v Biotin in 50% ethanol

Sulfur-Free Omerod's MMM
10% v/v 10X Sulfate-free Basal salts
10 mM NH_4Cl
0.015% v/v Biotin solution
0.1% v/v Vitamin Solution
30 mM DL-malate

PYE
0.3% w/v Peptone
0.3% w/v Yeast Extract
10% v/v 10X Sulfate-free Basal Salts
0.1% v/v Vitamin solution
0.015% Biotin solution
pH to 6.8 before autoclaving

LB
1% w/v Tryptone

0.5% w/v Yeast Extract
0.5% w/v NaCl

SOC
0.6% w/v Peptone
0.5% w/v Yeast Extract
0.058% w/v NaCl
0.0186% w/v KCl

Polymerase Chain Reaction Solution
20% v/v 5X GC Buffer (NEB)
3% v/v DMSO
0.2 mM dNTP Solution
400 nM Forward Primer
400 nM Reverse Primer
1% Phusion (NEB)
0.00008% Oligonucleotide-of-Interest

Polymerase Chain Reaction Conditions
Denaturation: 98°C for 30 s
Annealing: 62°C for 20 s
Extension: 72°C for 30 s per 1 kb of expected product length

7% Acrylamide Stacking Gel
7% w/v acrylamide
0.1575 M Tris pH 6.8
0.125% w/v SDS
0.025% w/v APS
0.0025% v/v EMED

12% Acrylamide Stacking Gel
12% w/v acrylamide
0.375 M Tris pH 8.8
0.1% w/v SDS
0.02% w/v APS
0.000125% v/v EMED